ADDIS ABABA UNIVERSITY

COLLEGE OF NATURAL SCIENCES

SCHOOL OF EARTH SCIENCES

THE ROLE OF SOIL AMPLIFICATION STUDIES IN SEISMIC HAZARD ASSESSMENT IN SOME SELECTED PARTS OF ADAMA TOWN, CENTRAL ETHIOPIA

BY

FREWEYNI MEKONEN

A THESIS SUBMITTED TO THE SCHOOL OF GRADUATE STUDIES OF ADDIS ABABA UNIVERSITY IN PARTIAL FULFILLMENT OF THE REQUIREMENTS FOR THE DEGREE OF MASTER OF SCIENCE IN EXPLORATION GEOPHYSICS

Addis Ababa

June, 2016

ADDIS ABABA UNIVERSITY

COLLEGE OF NATURAL SCIENCES

SCHOOL OF EARTH SCIENCES

THE ROLE OF SOIL AMPLIFICATION STUDIES IN SEISMIC HAZARD ASSESSMENT IN SOME SELECTED PARTS OF ADAMA TOWN, CENTRAL ETHIOPIA

BY

FREWEYNI MEKONEN

SCHOOL OF EARTH SCIENCES

Approved by Board of Examiners:	Signature	Date
Dr. Balemewael Atnafu Department Chairman and Department Committee	_____	_____
Prof. Tilahun Mammo Advisor	_____	_____
Dr. Abera Alemu Internal Examiner	_____	_____
Dr. Elias Lewi External Examine	_____	_____

ABSTRACT

Seismic hazard is one of the most destructive natural phenomena in the world as well as in our country. Subsurface conditions play a major role in the damage potential due to earthquake and seismic soil amplification of a site. The average shear wave velocity of the soil in the top 30 m layer is an essential parameter controlling the amplification behavior of a site. The present study was conducted in some selected parts of Adama town mostly in the northeastern and eastern part. The work was conducted to estimate soil Amplification and its role in seismic hazard assessment as well as the determination of the relevant parameters of site period and the average shear wave velocity to 30m depth(Vs30). Controlled source Seismic data was collected at 19 sites and analyses of seismic refraction and multi-channel surface waves data were conducted to examine the P- and S-wave characteristics of the subsurface. Depths to the bedrock and geological structures, average shear wave velocity to a depth of 30m, site periods and amplification factor values were calculated. Maps and graphs were produced to show spatial distribution of the various parameters. The research results suggest that the study area is under considerable danger of soil amplification.

Key words : Soil amplification, amplification factor, site period, shear wave velocity(Vs30) and site classification

ACKNOWLEDGMENT

First and foremost, I would like to thank the almighty God for the countless blessings and unlimited support.

I would like to express my deepest gratitude to my advisor Prof. Tilahun Mammo for his guiding, supervision, kind approach, encouragement and crucial comments that he provided throughout my research work. He has devoted his time, supplied relevant information, where his boundless support was indispensable to keep the research work.

I would like to say thank you to Dr. Abera Alemu and Prof. Tigstu Haile for their help in providing some valuable comments during proposal defense and sharing their research experiences during class.

It is my pleasure to thank PhD candidates Ato Geremew Lamessa for his limitless help and Ato Addis Eshetu.

I am also thankful to the School of Earth Sciences, Addis Ababa University, for the financial and equipment supports made to me for the present research work. I forward my gratitude to Dilla University which sponsored me.

My special thanks also goes to all my families members and friends for their support and encouragement during the period of the work.

TABLE OF CONTENTS

LIST OF FIGURES

LIST OF TABLE

ACRONYM

AF	Amplification factor
ASTM	American State Testing Materials
BH	Borehole
CMP	Common Mid Point
EAGLE	Ethiopia Afar Geosciences Lithospheric Experiment
EMU	Eastern margin unit
GIS	Geographic information system
H	Thickness
IBC	International Building Code
MASW	Multi Channel Surface Wave
MER	Main Ethiopian Rift
MM	Modified Mercali
NEHRP	National Earthquake Hazard Reduction Program
OWWDS	Oromia Water Works Design and Supervision
RRR	Rift- Rift- Rift
SMR	Southern Most Rift
SW	Surface Wave
T	Period
T-D	Time Distance
UTM	Universal Transverse Mercator
WFB	Wonji Fault Belt

CHAPTER ONE

1. INTRODUCTION

1.1 General

Seismic hazard is one of the most destructive natural hazard in the world as well as in our country. It is associated with an earthquake and have a potential to cause harm. There are factors which increase the damage of seismic hazard. Local soil condition or soil amplification factor is one of them, this can be investigated by different methods. In the present study soil amplification is obtained from shear wave velocity at 30m depth (Kramer, 1996).

Seismic hazard involving permanent ground displacement such as liquefaction, slope instability, subsidence, ground collapse, ground-motion amplification ,seismically induced soil settlements as well as seismically induced floods. In order to avoid these hazards seismic hazard assessment is very essential. In the assessment of the effect of various earthquakes soil amplification study plays a crucial role since once the seismic waves arrive at a given location, the local geology has great potential to modify the shaking and/or to modify to the shaking in such a way as to increase the potential for damage and injury.

Local geological conditions generate significant amplification of the ground motion causing damage during earthquakes. Usually the younger and softer soils amplify the ground motion more strongly than older and more consolidated soils. The soils (unconsolidated earth material, not bedrock) may also amplify the shaking. In ground motion soil layers cause significant amplification or enlargement and a long period of ground shaking (Habtom Gebremedhin ,2006).

The major effects to a site are due to seismic wave amplification caused by local unconsolidated sediments at specific frequencies during strong ground motions (Kuo, 2015). Recent studies of large destructive earthquakes have shown that damages during the earthquakes are often caused by the amplification of seismic waves in near-surface geology , where the post disaster damage assessment illustrated that the local soil effect may have a dominant contribution to the intensity of damage and destruction (Dabbeek, 2011).

The pattern of structural damage has been directly related to depth of soft alluvium overlying the bedrock.

Potential effects at allocation can be evaluated before an earthquake if good data are available on the thickness and nature of geologic materials or rocks and soils. The general rule is that sites underlain by softer soil material will be more affected than the hard rock sites from the starting point of geologic map, more and more refined interpretations of hazard are possible. Information on the material properties of the soil and rocks below the ground surface is also useful (Habtom Gebremedhin, 2006).

The characteristics of shaking at a site depend on the source characteristics and change as they travel through their path to get to the site (Figure 1.1). The wave amplitudes generally attenuate with distance as they travel through the bedrock in the crust (i.e. path effect) and they are modified by the local soil conditions at the site(i.e. site effect).

The important property of the local soil conditions that influence ground shaking is the shear wave velocity. Although seismic waves may travel a longer distance through the bedrock than through the local soils, the influence of the local soil conditions can be significant. Generally foundation layers are like a filter for seismic wave propagation. Seismic waves in certain frequencies are damped and in others amplified.

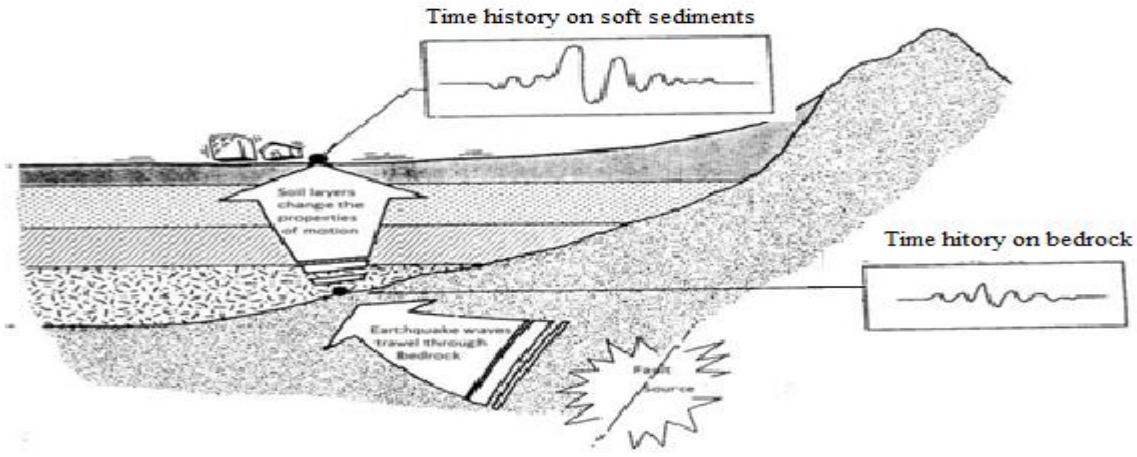

Figure 1.1 Propagation of seismic waves from source to surface source: (Navidi, 2012)

The effects of the local soil conditions on earthquake shaking are often quantified via an amplification factor. Investigations based on the observation and analyses of seismic ground motion have discovered that the average S-wave velocity of ground surface to a certain depth shows strong correlation with the relative amplification factor (Scawthorn, 2000).

Increase in ground motion intensity is due to dynamic response of local soil layers. Soil amplification effect is typically applied to "rock" ground motions defined by seismic hazard assessment. Soil amplification depends on soil properties and site period. Ground motion at a particular site can be influenced by the following conditions: Source, path and site

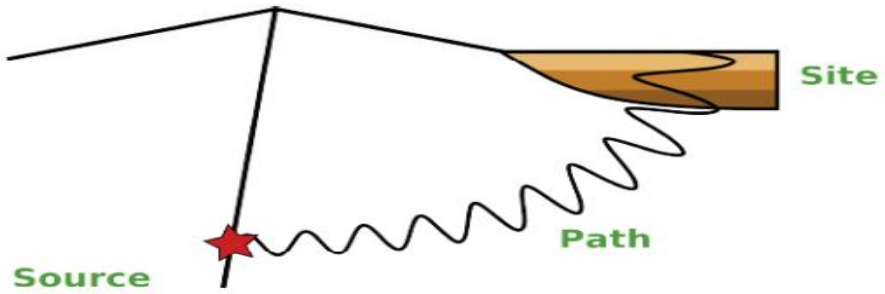

Figure 1.2 Ground motion at a site Source : Rathje , 2010, http://nees.org/resources/strata

Ground motion = Source ∗ Path ∗ Site

Source describes how the size and nature of earthquake wave generates or source controls the generation of earthquake wave. Travel Path explains the effect of the earth on waves as they travel. Local Site illustrates the effect of the upper most several 100metres of rocks , soils and surface topography at that location on the resultant ground motion produced by the emerging or passing earthquake waves. The Site term is given in terms of frequency-dependent amplification A(f) and diminution D(f) factors as

$$\text{Site}(f) = A(f) * D(f)$$

A simple way to characterize the soil conditions is by estimating the shear wave velocity of the deposit. The average shear wave velocity of the top 30 m i.e., $(V_s)_{30}$ is the most widely used

parameter to predict the potential amplification of sites during ground shaking (Maheswari et al, 2010).

1.2 Description of the study area

1.2.1 Location

Available documents evidenced that the study area, Adama had been known as Nazreth (the name given to it by Emperor Haile Sellasie I) for most of the 20th century up until it was officially reverted to its original Oromo language name, Adama, in 2000. Adama is located at about 100km from Addis Ababa towards southeast direction, in central Ethiopia. It is bounded by geographical UTM coordinates of 530000 to 537000m east and 941000 to 950000m north. The total area is 63km^2 . It is found in the central part of the Main Ethiopian Rift, which is cited in the Upper Valley of the Awash Basin within the East Shoa zone of Oromia National Regional State.

Adama is situated within the Wonji Fault Belt, in the main structural systems of the Ethiopian Rift Valley. According to Messay Mulugeta (2010), The major proportion of the City lies in a relatively low lying flat land (within 1 to 10% slope) between two mountain ridges, at an average altitude ranging between 1600 and 1970 meters above sea level. The annual rain fall of the area ranges between 700mm and 900mm.The annual temperature is about 20 degree centigrade with maximum temperature slightly exceeding 30-32 degree centigrade during May. The city sits between the base of an escarpment to the west and the Great Rift Valley to the east.

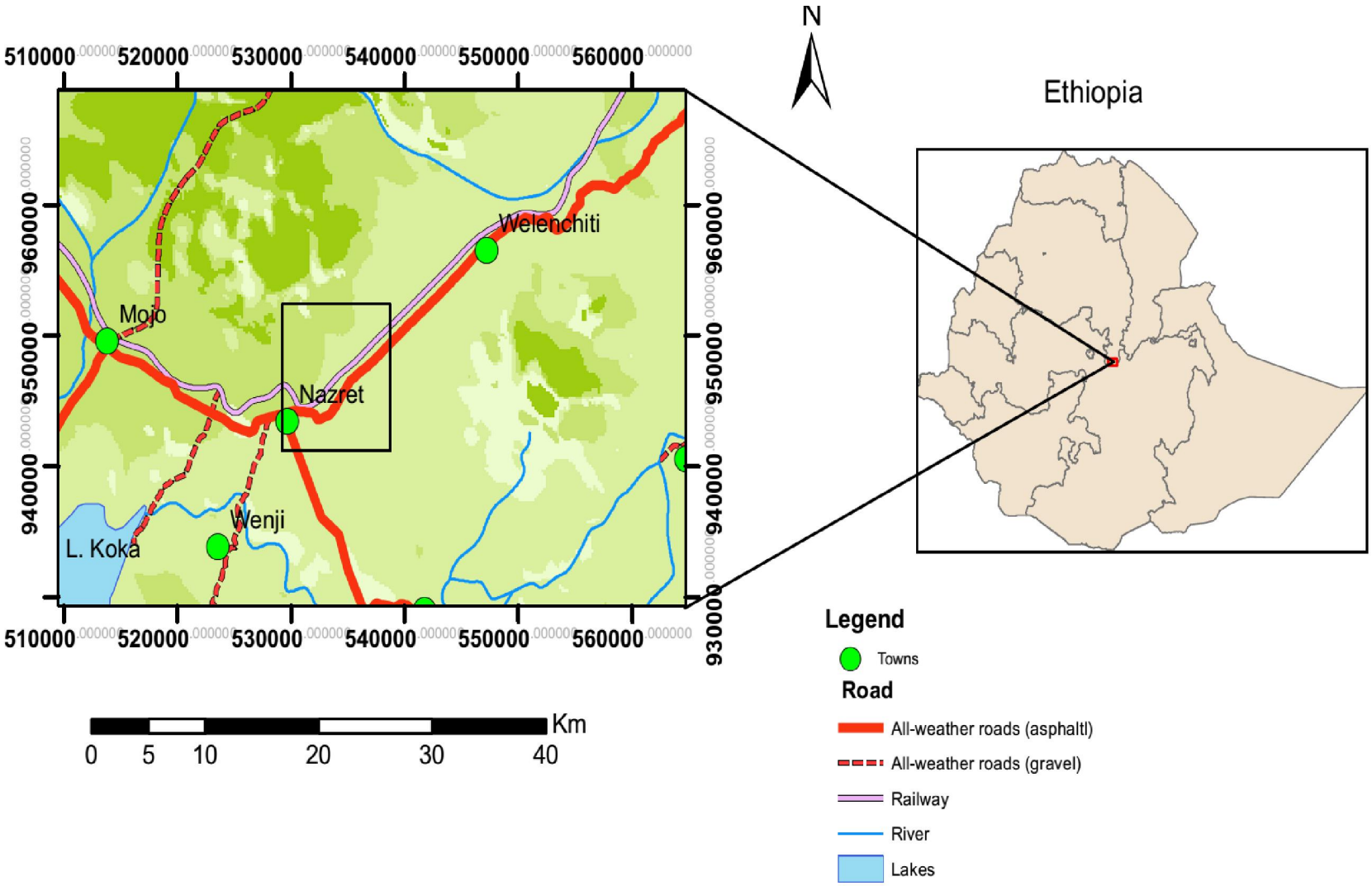

Figure 1.3 Location map of the study area and the rectangle shows the specific study area

1.2.2 Geomorphology

The study area is characterized by flat land that is surrounded by ridges. Different geomorphologic processes have been occurred in the area. These are production, movement and deposition of sediments. The primary responsible agents or driving forces for these processes are rain splash, wind erosion gulling due to earthquake and flooding etc. Due to this reason the plain land is covered by thick lacustrine sediments and reworked volcanic rocks. While the ridges are made of volcanic rocks.

Further geological studies indicate that the present land form of the area is the result of volcano-tectonic activities occurred in the past. The deposited of sediments in the area are mostly fluvial and lacustrine origin. Therefore, the landscape of Adama town consists of mostly flat lands which are covered with sediments and it is surrounded by ridges .Generally Adama town have graben characteristic feature (structure) .

Figure 1.4 Partial view of site

1.3 The Research Problem

Ethiopia's many cities like Addis Ababa, Adama(Nazret), Dire Dawa and Awassa are very near to main fault lines such as Wonji fault, Nazret fault, Addis-Ambo-Ghedo fault and Ful Woha fault lines. These towns suffered Earthquakes of different magnitude over the past years. There were a total of 16 recorded earthquakes of magnitude 6.5 and higher in some of Ethiopia's seismic active areas in the 20^{th}century alone (Fekadu Kebede, 1997).

In Ethiopia during the past 50 years there have been a dramatic increase in Urbanization related with increasing population. This results quick growth in the number of high rise buildings, residential house, schools dams, bridges, water supply pipes and other infrastructure constructions. The rapid growth in the number of existing constructions are expanding in size. Such new development imply increasing seismic hazard vulnerability of engineering structures and population centers. Therefore to minimize the effect of future damaging of seismic hazards in these Cities seismic hazard assessment is vital.

Therefore, the closeness of the significant Earthquake centers to Addis Ababa, Adama, Dire Dawa and Awassa which are some of the major population center, lead to the question of how much damage will be sustained by these buildings, bridges, dams etc. Majority of the buildings that are being constructed in the area were not well designed as per the harsh earthquake design guidelines and could not sustain significant damage varying from total collapse to structural failure (Fekadu Kebede, 1997).

Besides this, Adama is one of the fastest growing cities in the country and there is a big volume of construction works. Because it is the transit way on the road from Addis Ababa to Djibouti, the growth of trade and commerce is very high in the city. Different geological, hydrogeological, geophysical and seismic studies under taken so far in the area, but soil amplification factor of the did not study. Seismic studies without considering the soil properties cannot give full information about the damage due to earthquake. The present work tries to study soil amplification and its impact on seismic hazard assessment.

1.4 Objectives of the study

1.4.1 General Objective

The main objective of this research is to conduct detail studies of soil Amplification and its role in seismic hazard assessment in some selected parts of Adama Town.

1.4.2 Specific objectives

The Specific objectives of this research are:

- To determine soil thickness and soil amplification for the area of interest.
- To determine dominant soil period and produce soil period map of the study area.
- To determine amplification factor values and prepare amplification factor map of the area.
- To produce an average shear wave velocity distribution map for the upper 30 meter depth.
- To classify the soil based on average shear wave velocity of the upper 30metre depth.

1.5 Methodology

The methodologies followed in the present work is based on the objectives formulated in the above section. Predicting soil response is an important step in estimating the effect of earthquakes since local ground conditions substantially affect the characteristics of incoming seismic wave during earthquakes. Soil response study is carried out using geophysical data (average shear wave velocity and seismic refraction methods) (Anbazhagan et al., 2010).The amount of ground motion amplification depends on wave propagation characteristics of the soil, which can be estimated from measurements of shear wave velocity (Kelly, 2006).The seismic refraction data were collected using different shoots along the profiles since it is for both s-wave velocity and Velocity of Rayleigh Wave. Secondary data like bore hole from Oromia water works, design and supervision and Engineering geological, Geohazard data and topographic map from Ethiopia Geological Survey were collected. The data were processed and interpreted using different software such as seisImager/SW and other mapping software's (Surfer, ArcGIS, Microcal origin 6., and etc.) The generalized Flow chart of methodological approach is described in (Figure 1.5).

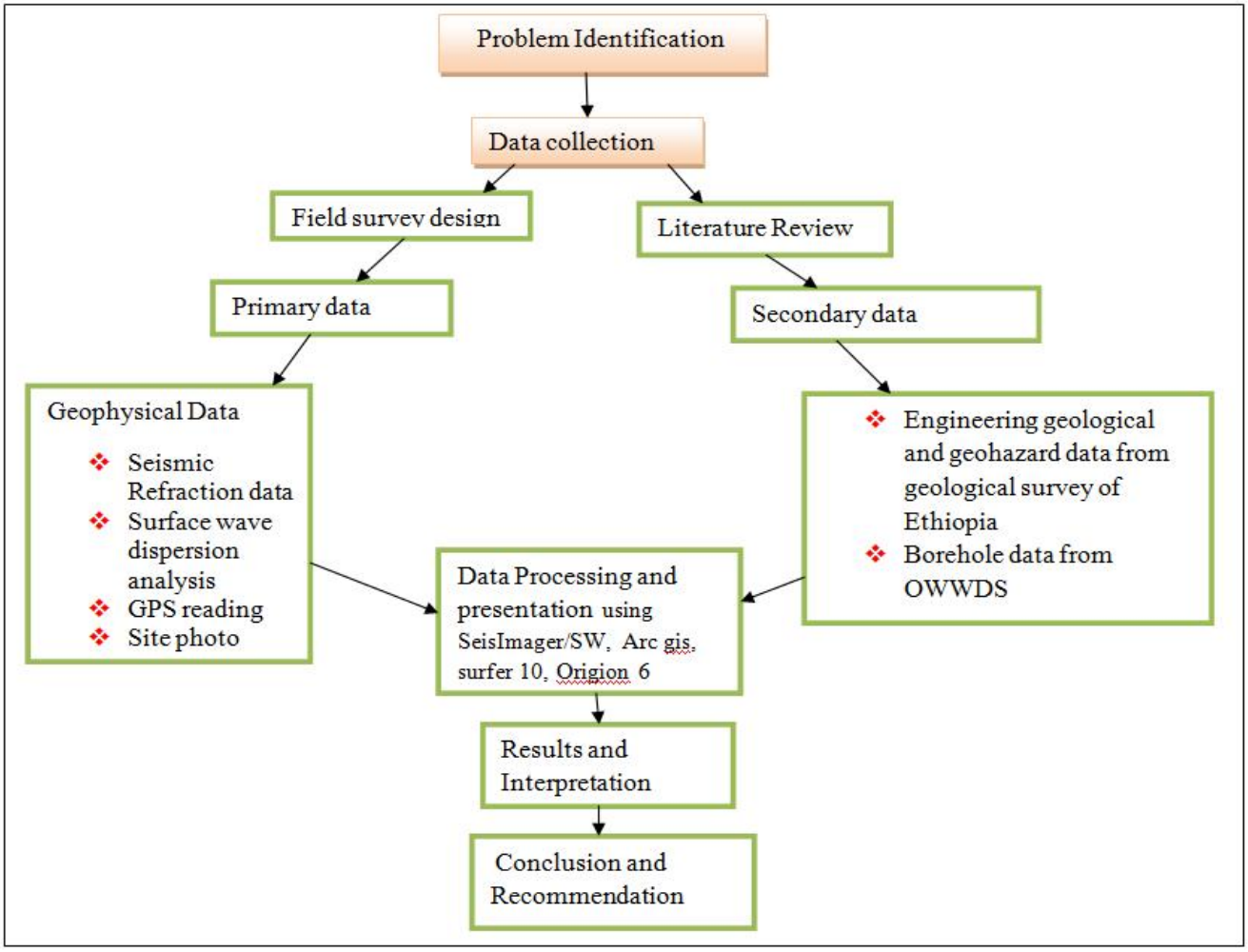

Figure 1.5 Flow chart of methodological approach

1.6 Significance of the study

The main aim of this study or engineering seismology is to ensure engineering structure safety. The present study together with previous geological and seismic studies made over the Adama area is expected to have the following outcomes:

- To build a safe or earthquake damage resistant and that are economically viable structures.
- To save life and properties from earthquake damage.
- To supply or contribute a scientific idea in the area for another researchers
- Helps to identify the most vulnerable localities in the area.

1.7 Previous Works

In the past many geological, geophysical, hydrogeological, geohazard and other related works have been performed for different purposes in the study area and its surrounding. A number of works have been done by different scholars. Some of the relevant works are:

- Arifi et al. (2012) made a study entitled Time Independent Seismic Hazard Analysis of the Afar depression. In this study the method they used is statistical method of estimation combines sample information and they got the highest values of the exceedance probability for intensity VII are relatively scattered, showing spatial distribution that conforms with the RRR (rift-rift-rift) relative translational and rotational motions of the three bounding (Main Ethiopian Rift-Southern Red Sea Rift-Gulf of Aden Rift)
- Mackenzie et al. (2005) conduct a systematic study on the Crustal velocity structure across the Main Ethiopian Rift: results from two-dimensional wide-angle seismic modeling
- Tigistu Haile et al. (2000) conducted an organized study on the geophysical, geological and hydrogeological investigations of Boku thermal field
- Habtom Gebremedhin (2006) performed a systematic study on earthquake hazard assessment in the main Ethiopian rift in Semera town by using remote sensing and GIS techniques
- Tigistu Haile et al. (2004) made integrated geophysical investigations to Study thermal zones at Boku volcanic Center, main Ethiopian rift

1.8 Layout of the Thesis

This thesis is organized in to six chapters. The first chapter is general introduction of the study. The second chapter is concerned mostly with the work of previous researchers that includes Seismicity, Tectonics, Basics of soil classifications, geological review and geology and structures of the study area. Chapter three covers the theoretical background of the seismic methods employed in this study. Chapter four describes the complete survey procedure, data acquisition, data processing, and presentation of the different results. Chapter five covers results and interpretations of seismic methods. The last chapter contains conclusions and recommendations of the research work.

CHAPTER TWO

2. GEOLOGICAL, SEISMICITY AND TECTONICS REVIEW

2.1 Regional Geology

Adama is found within the MER. The tectonic evolution of MER has been normally shared with pure and active extension mechanism (Mohr, 1983). The MER is characterized by a series of normal faults in most part of its margins and the youngest part of MER which is the axial zone or the floor of the rift is marked by narrow belt of active faulting and volcanism and is referred to as Wonji Fault Belt (WFB) (Mohr, 1967; Boccaletti et al., 1998, 1999). Caldera structures are other common tectonic features in the floor of the rift.

The MER is divided in to two according to structures: the Nazret-Dera area and the Asela-Ziway area. Since Adama is found in the Nazret-Dera area, it is used as a regional geology for this work. According to Alula Damte (1992) the volcanic succession outcropping in this area is subdivided into eight major units and the Boseti Volcano.

2.1.1 Eastern Margin Unit (EMU)

This unit covers the south-eastern corner of Nazret-Dera area, composed of alkaline basalts and ignimbrites, representing the pre-Wonji series products. Which contains series of basaltic lava flows, inter bedded with generally well welded ignimbrite sheets and somewhere with thick (1-1.5m) paleosoils. The rocks contain alkaline transitional basaltic lavas and pantelleritedacitic and rhyolitic ignimbrite sheets generally with green abundant matrix and usually of glassy dense “fiamme” and sporadic lava domes. Age determination for this unit is 1.8Ma (Bigazzi et al., 1993).

2.1.2 Nazret Unit

This unit consists of ignimbrite and basalts units. The ignimbrite unit show different degree of welding. They are much welded at the base containing large dense dark fiamme and a glassy matrix and loose at the top. The glassy fiamme have pantelleritic composition. The glassy matrix generally has abundant basaltic lithic fragments. The relative age for this unit is 1.7-1.5Ma. (bigazzi et al.,1993).

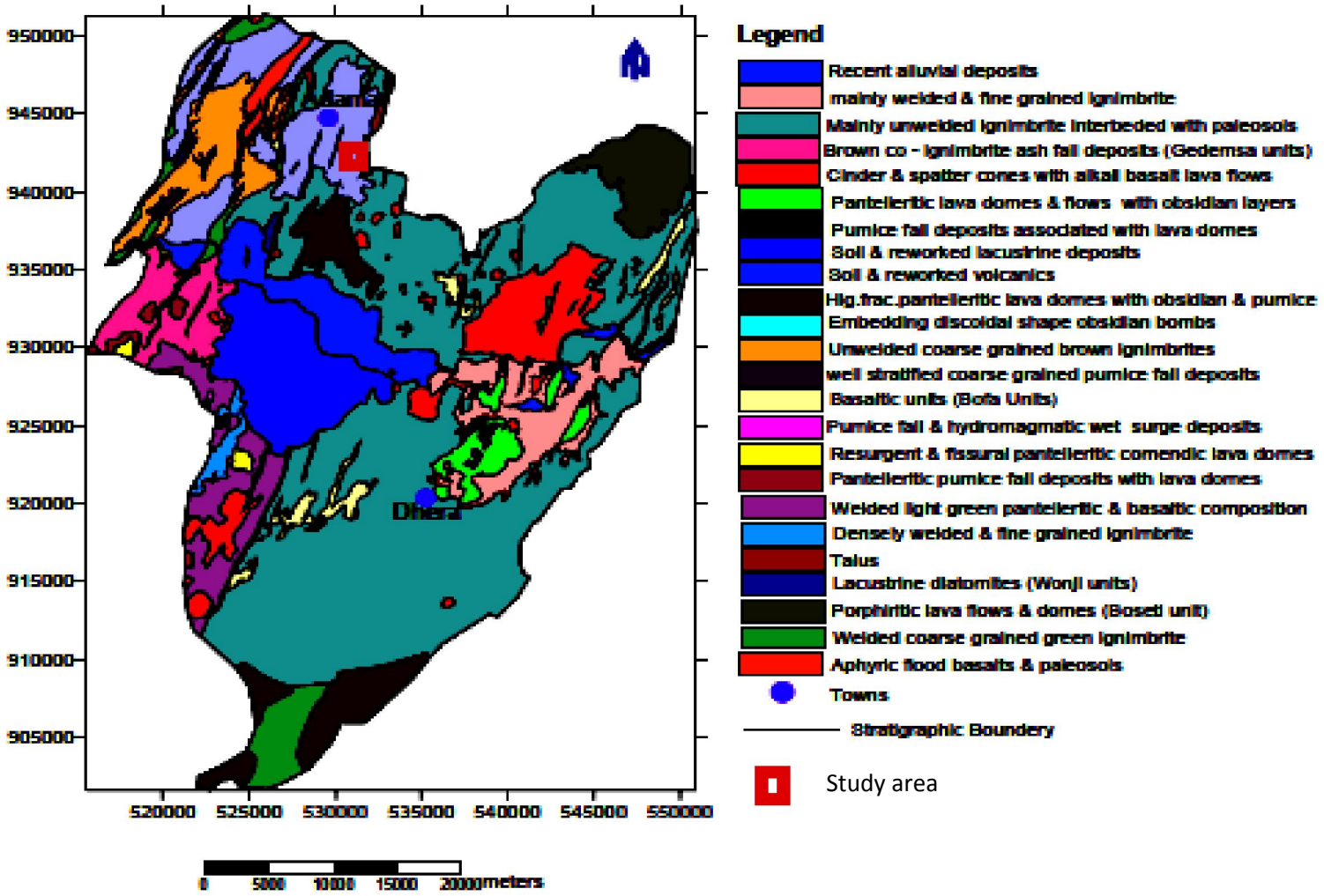

Figure2.4 Geological map of Nazret-Dehra area, Source : Alula Damte (1992).

2.1.3 Keleta Unit

These products are mainly wide spread on the south eastern sector of the Nazret-Dera area and could be considered as the actual rift floor refilling. They were erupted after a period of scarce volcanic activity marked by the presence of important layers of paleosoils. These products are characterized by a sequence of ignimbrite units that reach their maximum thickness (50-70m) in the Keleta river valley. The basalt units contain abundant lithic blocks with maximum diameter of 1-2m in the Keleta River valley (Bigazzi et al., 1993). The Keleta unit constitutes the basalt series of the so-called "Wonji series" (Meyer et al.,1975). This succession uncomformably overlies the previous Nazret unit products as well as the EMU.

2.1.4 Boku-TedeUnit

This unit relates to felsic products that linked to collapse of a relatively large caldera set in the central part of the Nazret-Dera area. The rims of the caldera are at present eroded and fragmented by tectonics. They contain ignimbrite sheets showing different degree of welding, pyroclastic fall, surge deposits and highly autobrecciated lava domes at places associated with banded obsidian lavas. The radiometric age determination available on rhyolite lavas and ignimbrites gave an age ranging from 0.83-0.51Ma (Bigazzi et al., 1993)

2.1.5 Bofa-Unit

It contains mafic lava flows and is mainly found in the central sector of the rift and overlying the ignimbrite succession of the Keleta. The lavas of this unit are commonly porphyritic for large boards of plagioclase. The thickness (30-50m) of the basaltic lava flows decreases from north east to the south west in the central sector of the rift. The radiometric ages range from 0.61 to 0.44 Ma (Bigazzi et al., 1993)

2.1.6 Dera-Sodere Unit

This unit contains the most widespread ignimbrite sheets and it covers 300 km^2. They are characterized by thin unwelded or poorly welded ash flows containing small scattered rounded pumice clasts and lithics in a fine grained abundant matrix. There are thin Paleo-soils at places inter bedded with the ash flow layers. The lavas of this unit are usually vesicular with scarce obsidian layers. The fine grained ash flow overlays the Bofa basalt. Age determination of these products is not available (Bigazzi et al., 1993).

2.1.7 Gedemsa Unit

This unit is described by felsic products and is related to the formation of a caldera. It extends towards the south-west of Boku along the central western sector of the rift. With around 8km diameter; the rims reach the maximum height (250-300m) in the north-eastern sector. The pre-caldera products are represented by pantelleritic ignimbrites associated with ash flows pumice falls and surge deposits and by pantelleritic lava domes. The post-caldera products are constituted by resurgent pantelleritic lava domes mainly placed inside the caldera floor. Basaltic spatter and cinder cones are found both inside and on the caldera rims. Since basaltic magmas were erupted in the area during and just after the volcanic activity that gave rise to the Gedemsa products. The age determination of this unit is 0.21Ma (Bigazzi et al., 1993).

2.1.8 Melkasa Unit

The most recent volcanic activity of the Rift gave rise to a series of spatter and cinder cones with associated tabular lava flows. These products are located in the central sector of the rift and they are particularly abundant in the south western sector of the Nazret-Dera region. Age determination for this unit is less than 0.2Ma (Bigazzi et al., 1993).

2.2 Geology and structures of the project site

2.2.1 Geology

The major part of the study area is topographically flat and is covered by Lacustrine sediments. Whereas some parts are covered by ignimbrite, ash flow tuffs and unwelded tuffs, rhyolite domes and flows, and basalt unit.

2.2.1.1 Lacustrine sediments

The lacustrine sediments in the rift proper comprise clay, silt, tuff, travertine, diatomite with intercalation of pumice. They are deposited from extensive lakes during Pleistocene pluvial, and are Pleistocene to Holocene in age (Getahun Kebede, 1987). They are exposed in almost all parts of the study area except in the southern and some selected parts. The thickness of lacustrine sediments reaches up to 18m in the eastern part. This unit covers about 56% of the area.

2.2.1.2 Rhyolite Domes and Flows

The rhyolite domes and flows are exposed in the central and northern part of the study area. This unit covers a small part of the study area (about 15%).

2.2.1.3 Ignimbrite, Ash flow Tuffs and Unwelded Tuffs

These are exposed in the southern and northern part of the study area. This unit covers up to 20% of the total area.

2.2.1.4 Basalt Unit

The basalt unit is exposed in the southern part of the study area. And this unit covers the smallest part of the study area 9%.

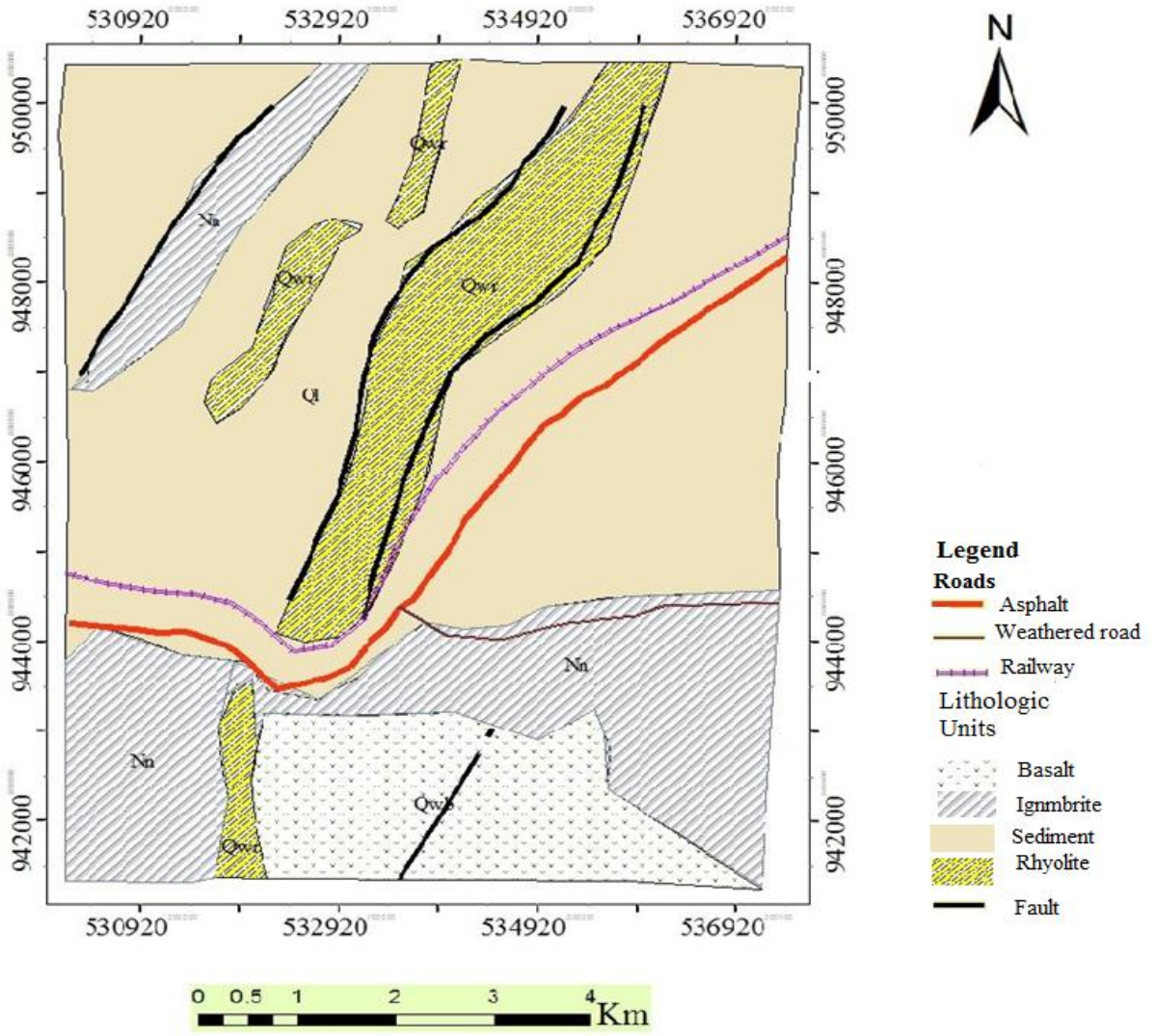

Figure 2.5 Geological map of the study area modified from:(Nazrate map sheet, 1978)

2.2.2 Structures

2.2.2.1 Fault

A fault structure is observed in the study area. It is normal fault because the hanging wall drops relative to the footwall as we see in the figure below. This fault is oriented from NNE to SSW direction.

Figure 2.6 Normal fault

2.2.2.2 Gully Structure

Gully erosion are also observed in the study area. The gully erosion extends in very large area in the Eastern part of the study area with depth ranging between 14 and 18 m (Figure 2.7). From this it can be conclude that the soil deposit is very thick.

Figure 2.7 Gully erosion

2.3 Seismicity and Tectonics of Ethiopian Rift System

Earthquakes have been a fact of life in Ethiopia for a very long time, because of its location is right on some of the major tectonic plates in the world, i.e. the African and Arabian plates. The earliest record of such earthquake dates as far back as A.D.1431 during the reign of Emperor Zara Yaqob (Gouin, 1979). In the 20th century alone, a study done by Pierre Gouin suggests that as many as 15,000 tremors, strong enough to be felt by humans, had occurred in Ethiopia proper and the Horn of Africa (Gouin, 1979).

According to the Ethiopia Building Code Standard (1995), The country is divided into five zones approximately equal seismic risks depending on the known distribution of earthquakes. These zones are no damaging zone (0 zones), less damaging zones (zone 1 and 2) and zones of major damaging (zone 3 and 4). From the seismic hazard map of Ethiopia, the project site falls in zone three as shown in Figure 2.1. This map is based on the amplitudes of the ground acceleration to be expected during 100 years return period. According to the building code, the ground acceleration ratio (α^0) depends on the seismic zones (see Table 2.1).

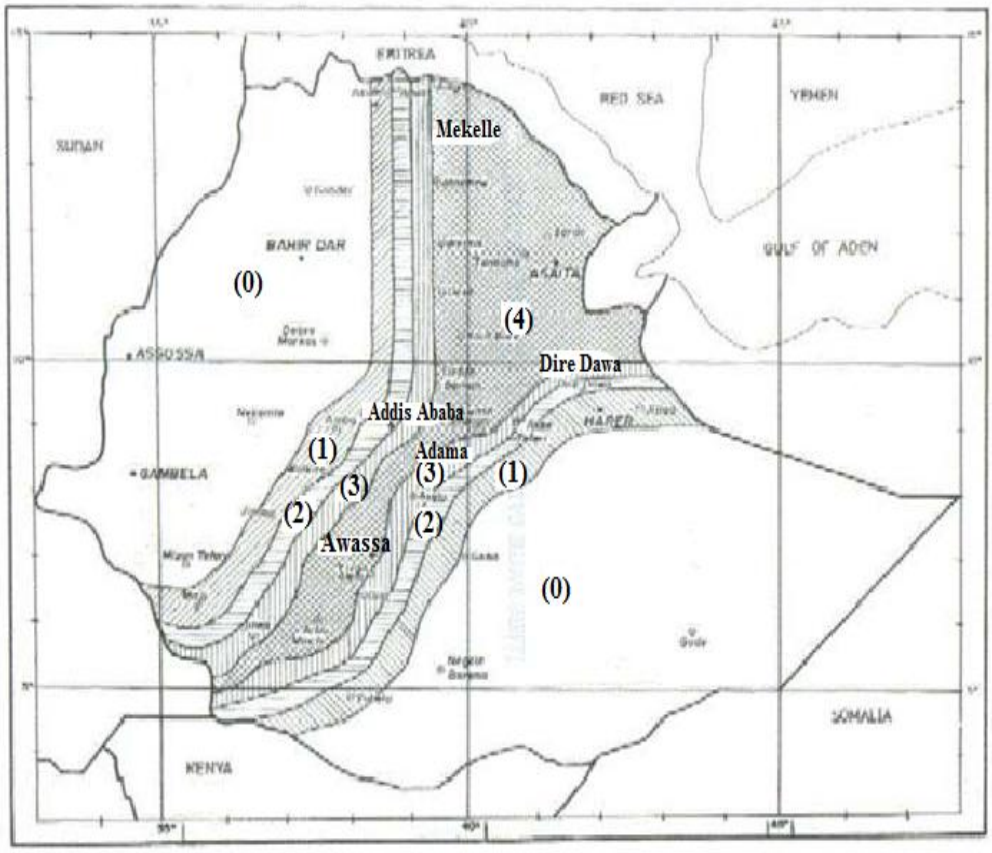

Figure 2.1 Seismic hazard map of Ethiopia (Ethiopian Building Code Standards, 1995)

Table 2.1 Bedrock acceleration ratio

Zone	4	3	2	1
α^0	0.10	0.07	0.05	0.03

Another study made by Fekadu Kebede (1996) indicated that there were a total of 16 recorded earthquakes of magnitude 6.5 and higher in some of Ethiopia's seismic active areas in the 20^{th}century alone. The most significant earthquakes of the 20^{th} and 21^{st}centuries like the 1906 Langano earthquake, the 1961 Kara Kore earthquake, the 1983 Wondo Genet earthquake, the 1985 Langano earthquake, the 1989 Dobi graben earthquake in central Afar, the 1993 Nazret earthquake, and the 2011 Hosanna earthquake were all felt in some of the major cities in the country such as Addis Ababa, Jimma, Adama and Awassa. In addition to Gouin's book that describes the earthquakes of 1906 and 1961 that shook Addis Ababa and caused widespread panic, a recently published Amharic biography of Blaten Geta Mersie Hazen Wolde Qirqos vividly describes the effect of the 1906 Langano earthquake in Addis Ababa and Entoto (Fekadu Kebede, 1996).

In addition to these seismic events many earthquakes have shaken the main Ethiopian rift (MER) and the southern rift valley of the country recently and now bringing the danger of seismic hazard. As human development activities in the areas which are close and within MER, the Afar Triangle and the South Rift Valley of the country is increasing, it is expected that the damage on property and loss of human life due to seismic hazard will increase very significantly.

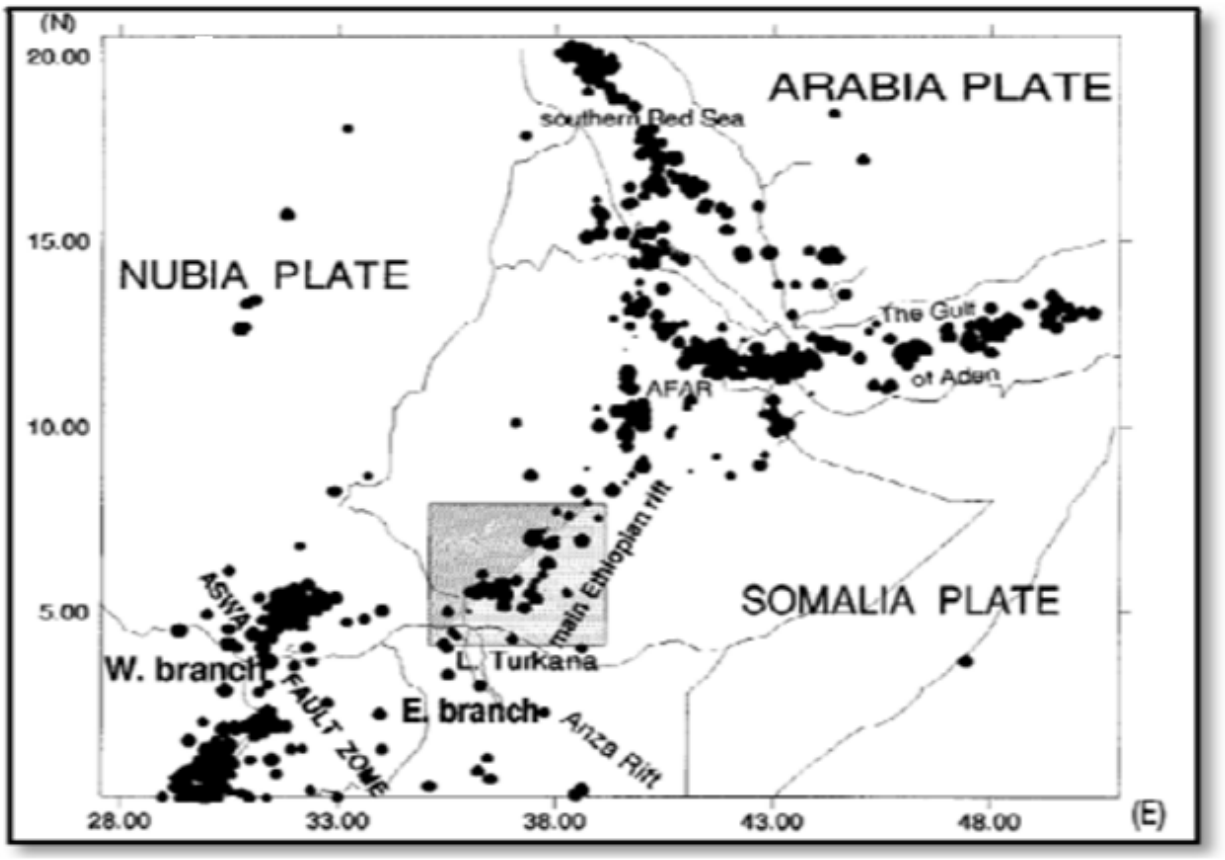

Figure 2.2 Seismicity of Ethiopia, with particular emphasis on the main Ethiopian Rift as well the Southern Rift Valley(Atalay Ayele,1995).The dots represent earthquake location.

According to Tilahun Mammo (2005) in terms of the mechanism that give rise to seismic hazard, the well accepted theory suggests a simplified model that typically considers three distinct seismic zones in Ethiopia. These are the Afar Triangle seismic zone(which further consists of the junction between Red Sea, Gulf of Aden, and the Main Ethiopian Rift), the Escarpment seismic zone(characterized by N-S running faults associated with some of the devastating earthquakes like the 1961 magnitude 6.7 Kara Kore earthquake) and the Ethiopian Rift System seismic zone this links to Red Sea Gulf of Aden East African Rift System through the Afar Triangle.

Another study made by Fekadu Kebede and Laike Mariam Asfaw (1996) is based on recent data and recent developments in the understanding of the tectonics of the region. They proposed a more complicated model consisting of eight unique seismic zones in proper Ethiopia and its surroundings as main contributors of damaging earthquakes. These are : the Awash shear zone in south Sudan (zone 1),the southernmost rifts(SMR) of the Ethiopian and Main Ethiopian Rift(MER) (zone 2), the western margin of Afar depression(zone 3),the Afar depression including Djibouti (zone 4), the region connecting northern Afar with axial trough of the Red Sea (Zone 6) the western of gulf of Aden (zone 7) and the Yemen extensional tectonic region(zone 8).

Newer studies regarding the seismicity of the region contribute better understanding of seismic in the country. For example the Ethiopia Afar Geoscientific Lithospheric Experiment (EAGLE) was carried out between 2001-2003 to explore the kinematics and dynamics of continental breakup using broadband seismic array.

2.4 Seismicity of The Project Site

Adama is located in high risk zone where earthquake with Modified Mercali(MM) intensity of VI to IX and the resulting acceleration of 0.04 to 0.12g is expected to occur in 100 years return period. Design of civil engineering structures to be made in the study region should be based on assumption of a realistic earthquake with a magnitude of M = 7 and intensity of IX MM that correlate with acceleration of 0.04 to 0.12g. Adama is regarded as seismically active area concerning earthquake hazards (Andargachew Haile, 2014).

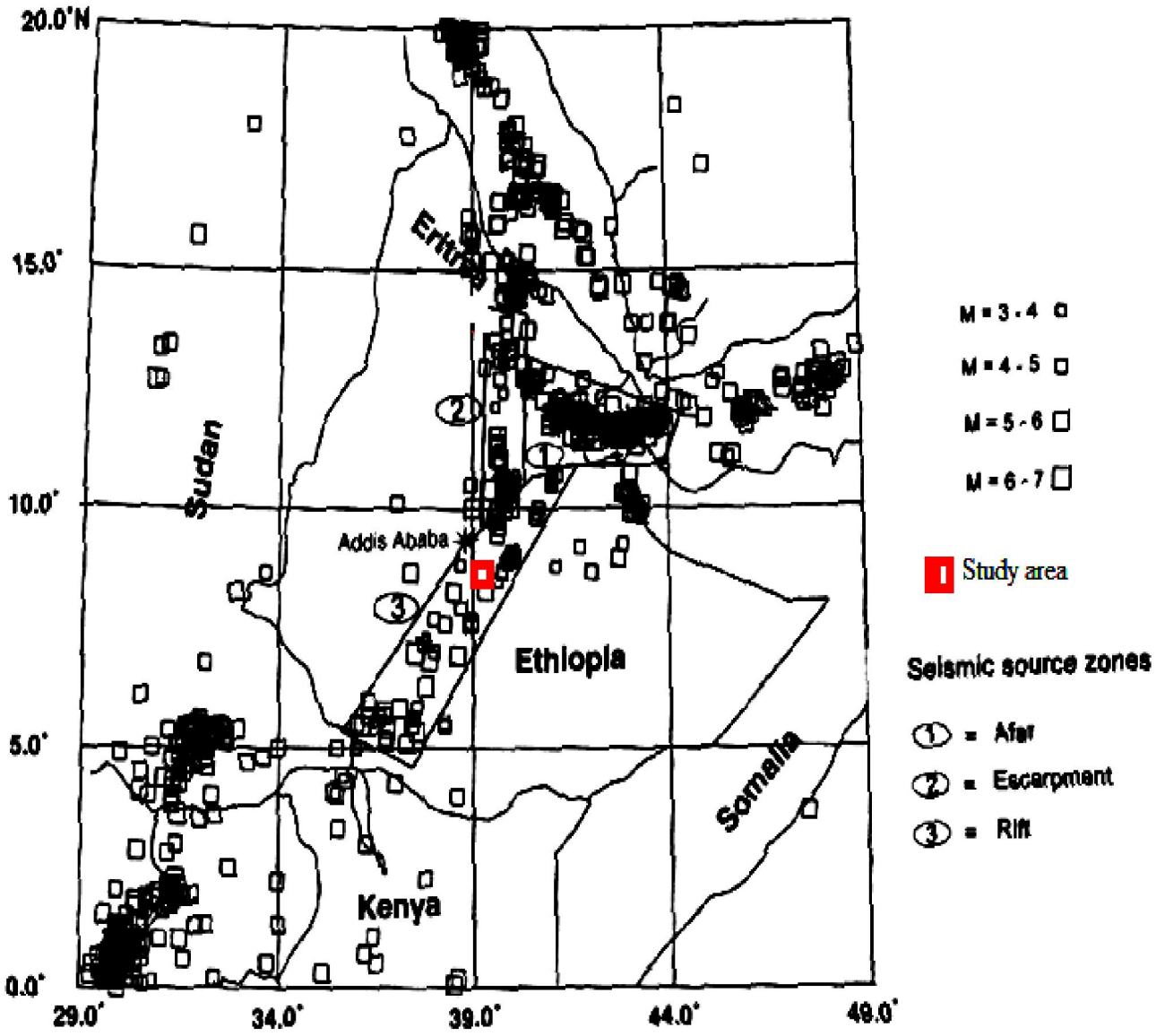

Figure 2.3 Seismicity of the region with the seismic source zones(Tilahun Mammo,2005)

2.5 Basis for Site Classification

Soils contain the products of physical and chemical weathering of the rocks of the earth's crust. Soil layers are in interaction with constructions and earthquakes. For example, the earthquake wave affects the soil strength characteristics, while soil strength characteristics also change the frequency, duration and amplitude properties of earthquake waves. The Vs shear wave velocity (if the thin layer in the surface is ignored) which has been obtained from the geophysical-seismic refraction measurements are used to study soil amplification. Shear wave velocity of soil layers

is a useful property for evaluating site amplification. Soil amplification was evaluated by empirical approaches based on shear wave velocity (Ferhat and Tazegul , 2011).

According to Dominic Kelly(2006) the source document for the site classifications defined in the IBC(International Building Code) is NEHRP(National Earthquake Hazard Reduction Program) recommended provisions for seismic regulations for new buildings and other structures. The amount of ground motion amplification depends on wave propagation characteristics of the soil, which can be anticipated from the measurements of shear wave velocity. Soft soils have slower shear wave velocity and generally produce greater amplification than stiff soils with faster shear wave velocity. The site classes of the IBC are defined in terms of shear wave velocity. Table 3.2 shows the site classification based on Vs30.

Table 2.2 the site classification, according to the NEHRP code

Site class	Average shear wave velocityVS30(m/s)	Remarks
A	Vs_{30}>1500	Hard rock
B	760≦ Vs_{30}≥ 1500	Rock
C	360≤ Vs_{30}≥ 760	Very dense soil and soft rock
D	180< Vs_{30} ≥ 360	Stiff soil
E	180 ≤ Vs_{30}	Soft clay soil
F		Soil requires site response analysis

The potential of seismic hazard depends on soil types. That means when the soil is soft ,thick and wet the damage due to earthquake increases and vice versa.

CHAPTER THREE

3. THEORETICAL BACKGROUND OF METHODS OF INVESTIGATION

3.1 Seismic Methods

3.1.1 Introduction

The basic principle of exploration seismology is for signal to be generated at a time that is exactly known and for the resulting seismic waves to travel through the subsurface media and be reflected and refracted back to the surface where the returning signals are detected. The elapsed time between the source and being triggered and the arrival of the various waves is then used to determine the nature of the sub-surface layers. The derived information is used to develop images of the subsurface structures and knowledge of the physical properties of the materials (rocks, soils etc....) present.

Exploration seismic methods were developed out of pioneering earthquake studies in the mid to late 19^{th} century. The first use of an artificial energy source in a seismic experiment was in 1846 by Robert Mallet, an Irish physicist, who was also the first to use the word seismology. There are two main seismic methods. these are refraction and reflection (Reynolds, 1997). Data supplied by Seismic methods are consistent and thorough in order to assess the seismic site characterizations and interpret the local site conditions particularly in calculating seismic hazards. Seismic methods have generate a considerable effort aimed at clarifying or measuring the soil conditions for ground motion calculation. These methods are an indicators of the potential for site amplification and classification of soils based on their shear wave velocity (Kockar, 2006).

3.1.2 Seismic Waves

Seismic waves are propagating vibrations that carry energy from the source of shaking out ward in all directions. Seismic waves are elastic waves that propagate though the medium without causing permanent deformation at any point in the medium. There are two major classes of modes of propagation or seismic waves: body waves which pass through the volume of a material and surface waves that exist only near a boundary. Body waves, or stress (seismic) waves propagating far from any boundaries in a uniform medium, two fundamental modes of propagation exist: compression waves also called P-waves, and shear waves also called S-waves.

Since they propagate within the mass or body of the medium, the waves are known as body waves (Kockar, 2006). Body waves are the fastest traveling of all seismic waves. The particle motion of P-waves is extension (dilation) and compression along the propagating direction. P-waves travel through all media that support seismic waves, air waves or noise in gasses, including the atmosphere, are P-waves. Compressional waves in fluids, e.g. water and air, are commonly referred to as acoustic waves.

The second wave type to reach a point through a body is the secondary or transverse or shear wave (S-wave). S-waves travel slightly slower than P-waves in solids. S-waves have particle motion perpendicular to the propagating direction. These transverse waves can only transit material that has shear strength. S-waves do not exist in liquids and gasses, as these media have no shear strength. Particle displacements are horizontal for SH-waves traveling in the vertical plane (U.S. Army Corps of Engineers, 1995).

The velocity of p- wave is:

$$Vp = \sqrt{\frac{k + \frac{4\mu}{3}}{\rho}} \qquad (3.1)$$

The velocity of s- wave is:

$$Vs = \sqrt{\frac{\mu}{\rho}} \qquad (3.2)$$

Where k = bulk modulus, μ = rigidity (shear modulus) and ρ = density

The ratio of velocity of p wave and s wave is known as Poisson‘s Ratio.

Seismic wave velocities of rocks: By virtue of their various compositions, textures (e.g. grain shape and degree of sorting), porosities and contained pore fluids, rocks differ in their elastic moduli and densities and, hence, in their seismic velocities.

Information on the compressional and shear wave velocities, Vp and Vs of rock layers encountered by seismic surveys is important for two main reasons: first, it is necessary for the conversion of seismic wave travel times into depths, second it provides an indication of the lithology of a rock or, in some cases, the nature of the pore fluids contained within it. Velocity of seismic waves of different earth materials are shown in the table below.

Table 3.1 Velocity of Body waves in different earth materials

Material	P wave velocity(m/s)	S wave velocity
Air	332	-
Water	1400-1500	-
Petroleum	1300-1400	-
Steel	6100	3500
Concrete	3600	2000
Granite	5500-5900	2800-3000
Basalt	6400	3200
Sandstone	1400-4300	700-2000
Limestone	5900-6100	2800-3000
Sand(unsaturated)	200-1000	80-400
Sand(saturated)	800-2200	320-880
Clay	1000-2500	400-1000
Glacial Till(saturated)	1500-2500	600-1000

In an infinite homogeneous isotropic medium, only body waves exist (Aki and Richards, 1980). However, when the medium does not extend to infinity in all directions, surface waves (known in seismic exploration as ground roll) can be generated. The primary type of surface wave is the Rayleigh wave. This wave travels along the surface of the earth and involves an interference of the P-wave and S-wave. The particle motion is confined to the vertical plane that includes the direction of propagation of the wave. The motion is counter clockwise (retrograde) at the surface, changing to purely vertical motion at a depth of about one fifth of a wavelength, and becoming clockwise (prograde) at greater depths.

The amplitude of the Rayleigh wave motion decreases exponentially with depth. Because of the existence of vertical medium-velocity gradients in the real world, the variation of the velocity of the Rayleigh waves with wavelength can be expressed using dispersion curves. Longer period waves travel faster because they sense the faster material at greater depth. The second type of surface wave is the Love wave. Love waves are formed through the constructive interference of high order SH multiples. The particle motion is horizontal and in the direction of SH waves. The amplitude of this wave motion decreases exponentially with depth. They exhibit dispersion as well.

Rayleigh waves often are dominant events in seismic records. The amplitude of surface waves decreases exponentially with depth. Most of the energy propagates in a shallow zone, roughly equal to one wavelength. Consequently, the wave propagation is influenced by the properties of this limited, near surface portion of the geological or geotechnical profile.

The propagation of surface waves in a vertically heterogeneous medium shows a dispersive behavior. Dispersion means that different frequencies have different phase velocities. The relation between frequency and phase velocity is called a dispersion curve and depends on the geology underneath. At high frequency, the phase velocity is close to the S-wave velocity through the uppermost layer. At low frequency, the effect of deeper layers become important, and the phase velocity tends asymptotically to the S-wave velocity of the deepest material, as if it extends infinitely in depth (the half space) (Pei, 2007).

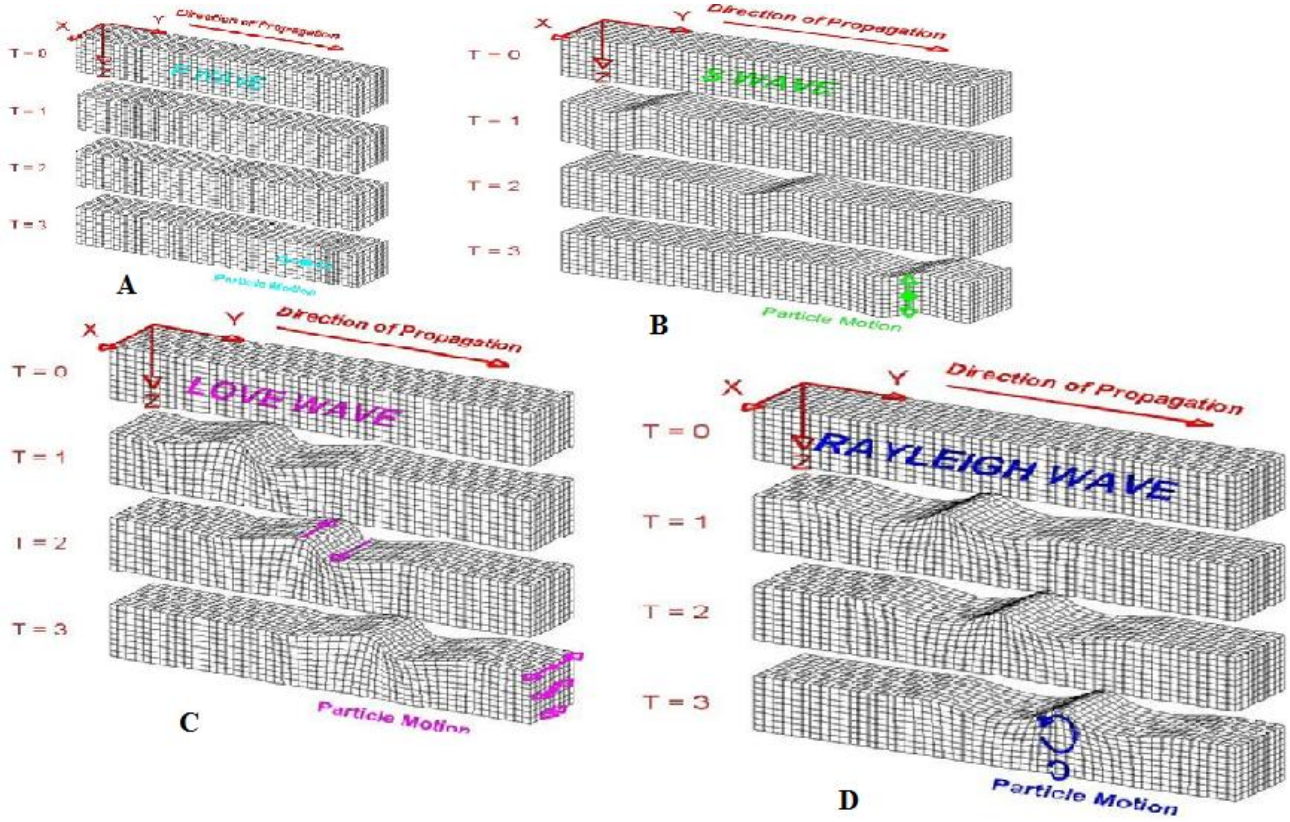

Figure 3.1 propagation of the waves A) P wave, B) S wave, C) Love wave and D) Rayleigh wave
Source : www.geo.mtu.edu/UPSeis/waves.html Michigan Technological University

3.2 Refraction Survey Method

This method is based on the ability to detect the arrival of wave energy that is critically refracted from a higher velocity layer underlying lower-velocity sediment. The test is performed by organizing a linear array of receivers on the ground surface, as shown in Figure 3.2 Refracted arrivals from energy traveling along interfaces below the exposed surface are used to measure the velocities of underlying layers. Although there are several types of seismic refraction methods depending on the survey objectives or targets that can be performed with both shear and compression wave energy, the most common methods are based on the first arrivals of P-waves (U.S. Army Corps of Engineers, 1995).

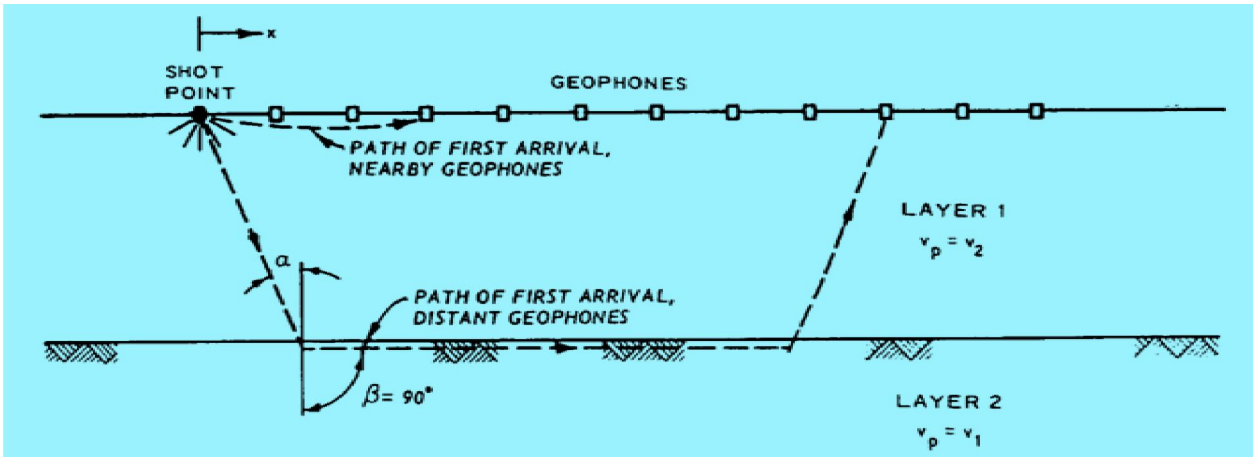

Figure 3.2 Schematic of seismic refraction survey

Shear wave refraction is more complicated to implement than compression wave refraction because the shear wave is a later wave arrival and may be masked by other wave arrivals in the time record. Therefore, the orientation and polarity of the source must be controlled to ensure that the shear wave is the dominant energy generated and received. It is preferable to generate and measure horizontally polarized shear (SH) waves to limit the conversion of shear-to-compression waves at soil interfaces which would further complicate the interpretation of wave arrivals (U.S. Army Corps of Engineers, 1995).

3.2.1 Instrumentation and Field Procedures

Geophysical equipment used for surface seismic refraction measurement includes a seismograph, geophones, geophone cable, an energy source, a trigger cable or radio link and metal plate. A wide variety of seismic geophysical equipment is available and the choice of equipment for a seismic refraction survey should be made in order to meet the objectives of the survey. With a multi-channel seismograph(i.e. 12 to 24 or more channels), the seismic wave forms are recorded simultaneously for all geophones. The simultaneous display of waveforms enables the operator to observe trends in the data and helps in making reliable picks of first arrival times and for analyzing S wave velocities.

A geophone transforms the P-wave energy into a voltage that is recorded by the seismograph. For refraction work, the frequency of the geophones varies from 10 to 28 Hz. The geophones are connected to a geophone cable that is connected to the seismograph as shown in the figure

below. The geophone cable has electrical connection points for each geophone, usually located at uniform intervals along the cable. Geophone placements are spaced from about 2 to 5m.

Energy Sources: The selection of seismic refraction energy sources is dependent upon the depth of investigation and geologic conditions. Four types of energy sources are commonly used in seismic refraction surveys: sledgehammers, mechanical weight drop or impact devices, projectile (gun) sources, and explosives. In the present the energy source is sledgehammer with a weight of 12 kg. A strike (metal) plate on the ground is used to improve the coupling of energy from the hammer to the soil. Trigger cable is used to make a connection between the sledgehammer and the seismograph and it converts mechanical energy in to electrical energy or it is used to initialize the recording by connecting directly with sledge hammer and the seismograph.

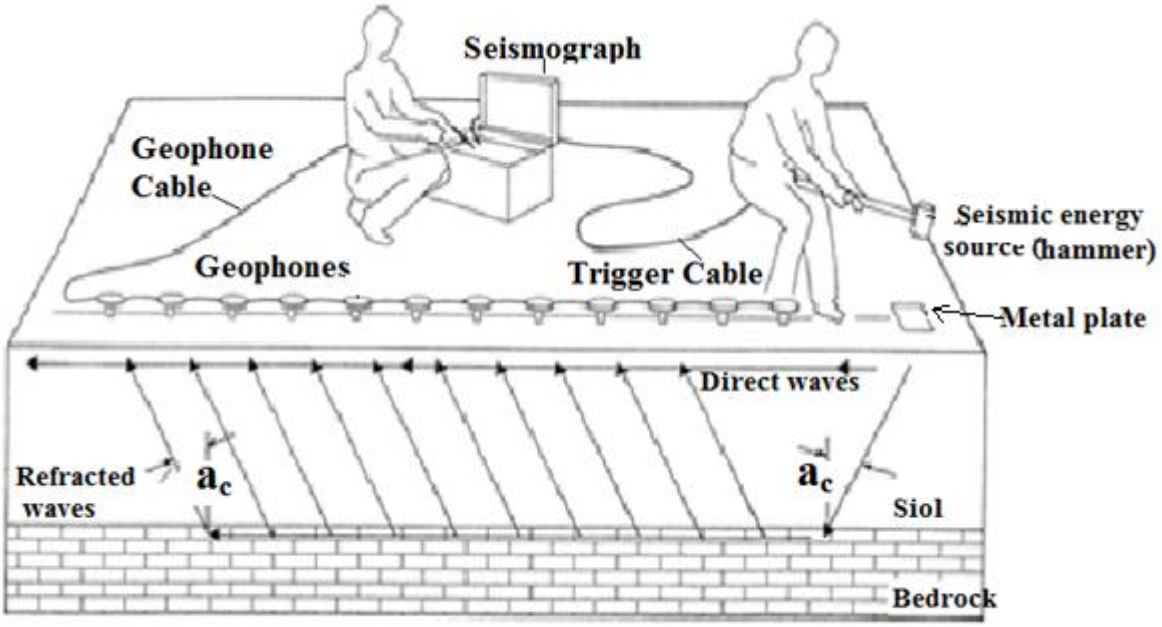

Figure 3.3 Field Layout of a multi-Channel Seismograph Showing the Path of Direct and Refracted Seismic Waves in a Two-Layer Soil/Rock System, α_c = Critical Angle (ASTM International)

The measurement of seismic shear waves is a subset of seismic refraction. Usually for amplification and site response study, the 30m average Vs is considered (Anbazhagan and Sitharam,2008).

CHAPTER FOUR

4. SEISMIC DATA ACQUISITION, PROCESSING AND PRESENTATION

4.1 Seismic Methods Employed

This research is done based on seismic refraction and Multichannel analysis of surface waves to identify the local site conditions and for predicting seismic soil response in some selected parts of Adama town.

To meet the objectives of the thesis and to determine the influence of the local geologic and soil conditions on the amplification of the seismic waves both the seismic refraction and surface wave dispersion analysis methods were employed. Both methods are supported to map the soil layers and depth to the basement. In addition, the methods measure the P- and S- wave velocities providing spatially averaged stiffness measurements of the soils.

4.2 Data Acquisition

Data acquisition for both refraction and surface wave analysis is based on a similar field layout and both data are simultaneously recorded. The equipments and materials used during the field work are shown in Figures 4.1 – 4.2. The multichannel signal enhancement Oyo McSEIS-SX seismograph with 24 vertical geophones of 5 meters spacing is used to collect good quality data in the noisy environment of the city. The acquisition parameters are shown in Table 4.1. The field procedure employed was an in-line spread in which the source and the geophones were placed in a straight line. The energy source is an 8 kg sledge hammer manually impacted on 150cm^2 metal plate to generate seismic signal. The source was activated at three different points (-30, 57.5, and 145 m) for the sixteen sites and at five different points (-30, -5, 57.5, 120 and 145 m) for the remaining three sites along the spread.

Table 4.1 Shows the data acquisition parameters

Parameter	Range
Recording system	McSEIS-SX 24
Format	SEG-2
Stack	Summation
Number of channels	24
Geophone spacing	5m
Sampling rate	200μs
Record length	
Receiver	28 Hz vertical (spikes or
Source	12 kg hammer (on metal
Offset distance	30 m

To generate the wave the plate was struck vertically in the direction perpendicular to the spread. The generated data were recorded at all shot points on an average of 8 to 13 stacks. Data collection was conducted at 19 sites (Fig. 4.3).

Figure 4.1 Instrumentation of seismic data acquisition

Figure 4.2 Schematic diagram of data acquisition process

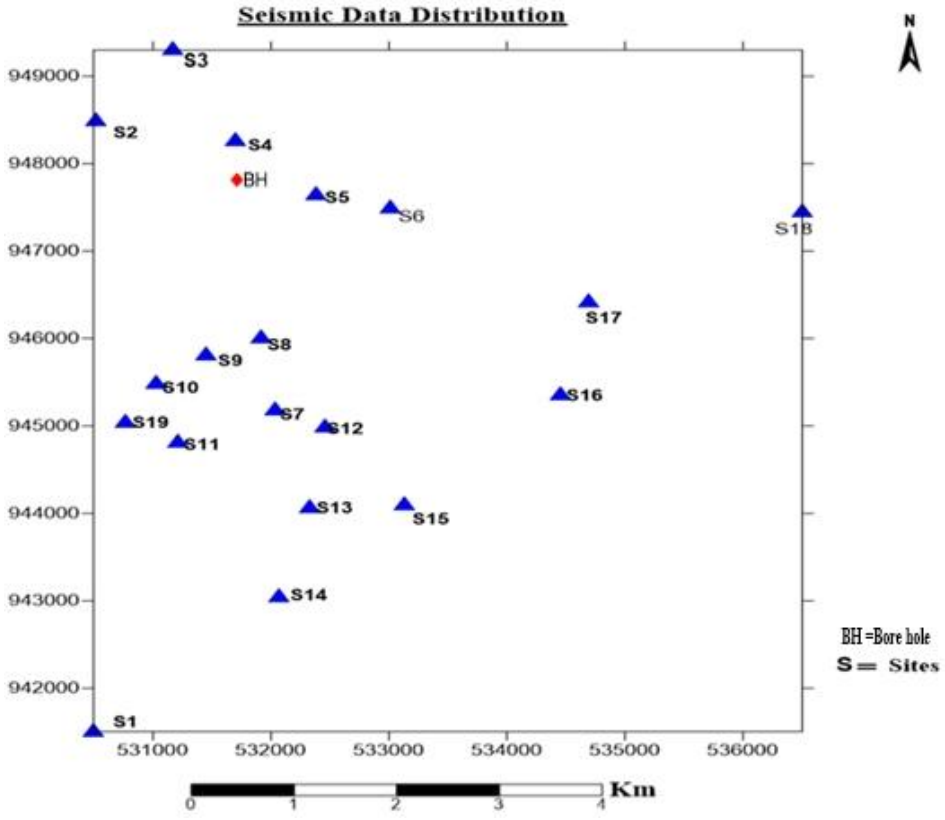

Figure 4.3 Seismic Survey data distribution and location in the study area

4.3 Data Processing

4.3.1 Seismic Refraction Data

The processing steps followed in this work are shown in Fig. 4.4. The waveform recorded in SEG-2 format is processed using SeisImager software. After editing for the bad and noisy data the first step conducted was to pick the first arrivals. Fig. 4.5 a,b show shot gathers with clear first-arrival onsets. The picking was done using Pickwin software. The time picks from all receivers together with the distance information are used to compute the traveltime curves using Plotrefa software (Fig. 4.5c). The parallelism of the traveltime curves is checked and ascertained for any irregularity and mispicking.

A particular traveltime T is given by a path integral through the medium as

$$T = \int_s \frac{ds}{v(s)} = \int_s u(s)ds \qquad (4.1)$$

where u(s) is the slowness [1/v(s)] along the path "s". The tomographic method requires an initial velocity model and is obtained from the Time Term Method incorporated into the software. After assigning the number of iterations and the required range of velocities the inversion process is launched. Rays are traced through a model made up of many cells and the velocities in each cell are changed to improve the fit until acceptably small errors are achieved between the observed and the predicted travel times.

$$\sum_j l_j \Delta u_j = \Delta T = T_{obs} - T_{pred} \qquad (4.2)$$

The ray tracing process calculates the travel times for the resulting model and calculates and plots the errors between the model and the data (see Fig. 4.5c).

The tomographic inversion in the end recovers the velocity model Δu_j from the observed travel times. The final 2D velocity model is shown with the raypaths superimposed (Fig. 4.5d).

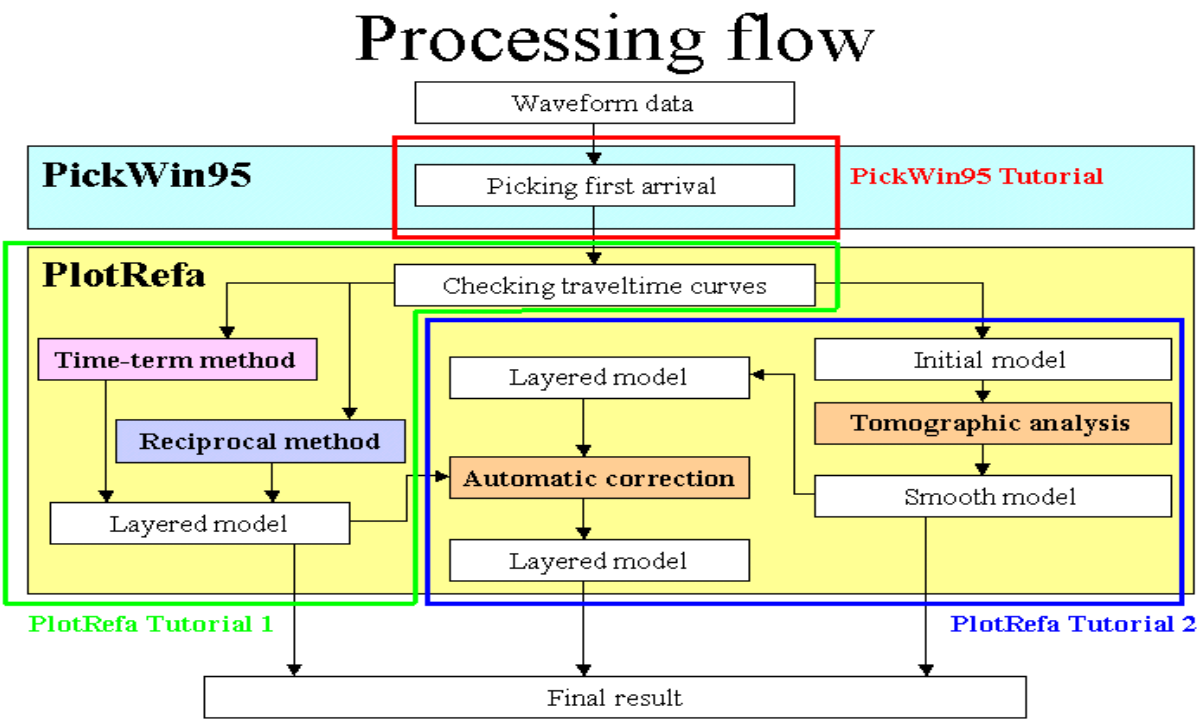

Figure 4.4 Flow chart of the Refraction seismic data processing

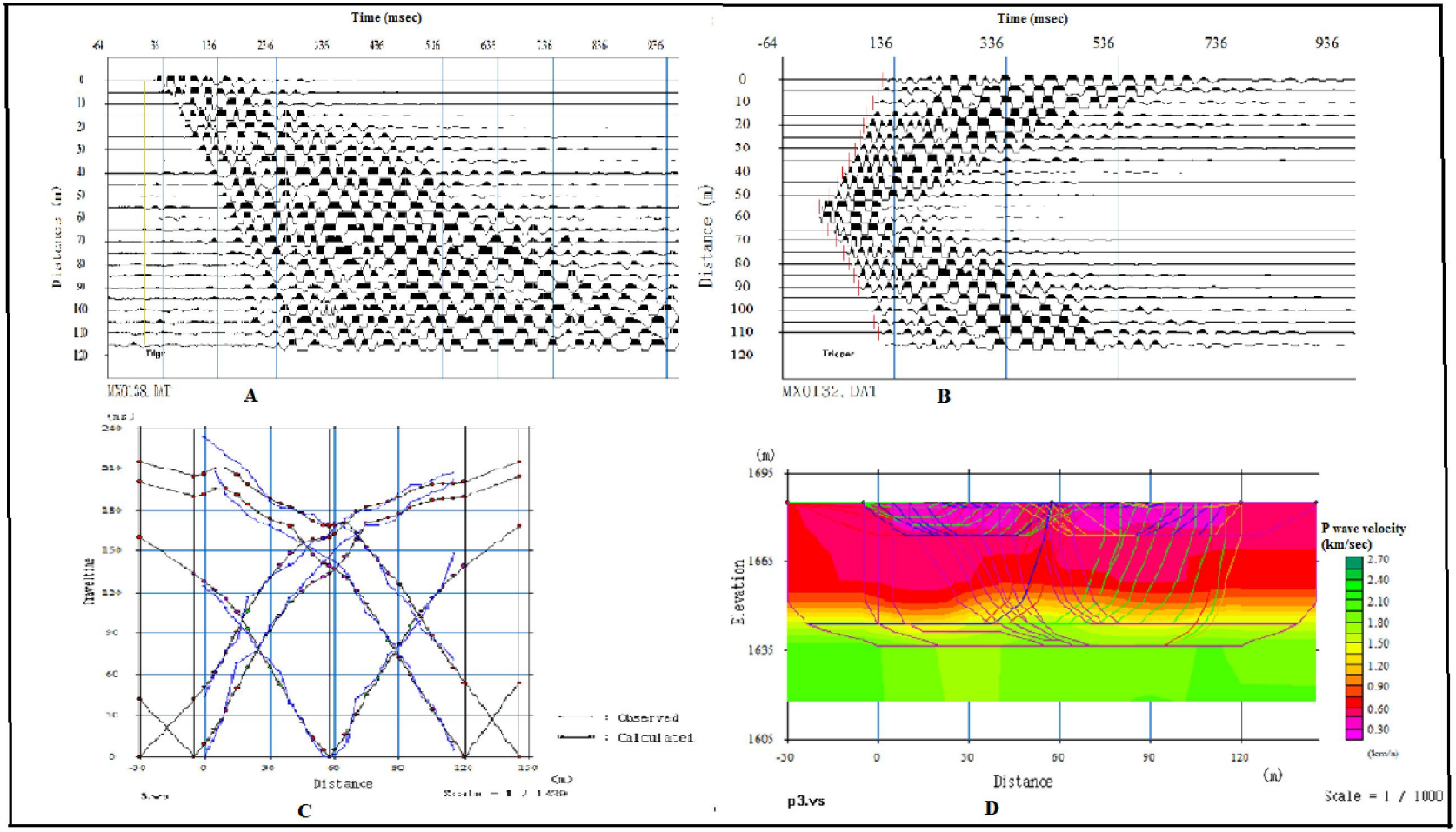

Figure 4.5 Seismic Refraction data processing and presentation (A=raw data or waveform, B=picked first breaks, C=travel time and D=ray paths and velocity model together)

4.3.2 Multichannel Analysis of Surface wave (MASW) Data

Surface waves travel at velocities that are controlled by their wavelengths. Longer wavelength, and hence lower frequency, waves penetrate deeper than shorter wavelength, higher frequency waves. In areas of varying velocity with depth, the relationship of frequency versus velocity for a surface wave train is called a dispersion curve.

The dispersive properties of surface waves can be used to obtain information related to the various layers and their elastic properties. Compared to the other seismic waves, surface waves have the strongest energy by virtue of which they have the highest signal to noise ratio and this makes it a powerful tool for near surface characterization(Kanli et al., 2006).

In the analysis of surface waves SeisImager/SW software has been used. Figures 4.6 and 4.7 shows the detailed steps which are involved in the analysis of surface wave data to obtain a two dimensional shear wave velocity models. The data processing consists of two main objectives: (i) to obtain the dispersion curves of Rayleigh wave phase velocity from the records and (ii) to determine the various layers and their shear wave velocities. From the shear wave velocities the average velocity to a depth of 30m, the $(V_s)_{30}$ values are calculated. This is because various studies reveal that it is the upper 30 m that is crucial for the determination of seismic wave amplification (Mohamed et al., 2013)

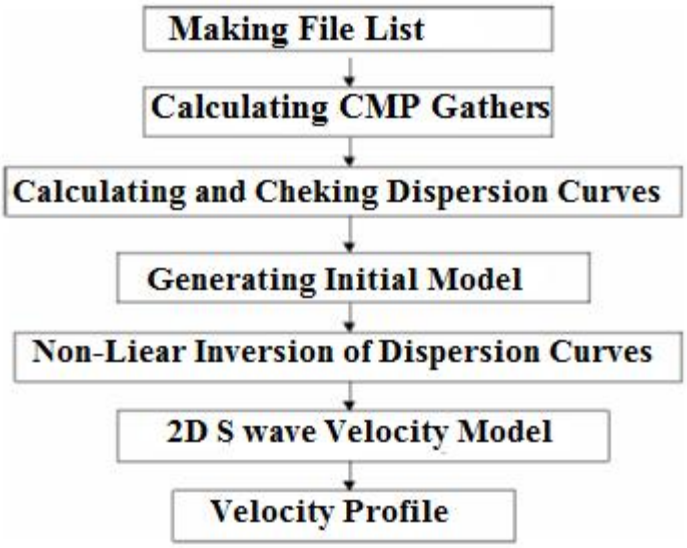

Figure 4.6 Flowchart for the analysis of surface wave data

The steps followed in the analysis of surface waves are as follow. The first step is to make the file list. In this step all waveform files and the source receiver configurations are mentioned and organized according to the field procedures and cross correlation Common Mid Point (CMP) gather is calculated. The dispersion curves are calculated by converting it into frequency domain.

The generation of dispersion curve is the most important part for generating an accurate shear wave velocity profile. The dispersion curves are displayed as frequency versus phase velocity. The Phase velocity relation can be calculated from the linear slope of each component on the swept frequency record. A shear wave velocity profile has been calculated using an iterative inversion process that requires the dispersion curve developed as input. And the initial earth model is specified to begin the iterative inversion process.

A 1-D average dispersion curve and the corresponding shear wave velocity profile was determined for each seismic source using nonlinear least squares (NLS) technique. The tomographic inversion code was then used to reconstruct a 2-D velocity field as shown in Fig. 4.7

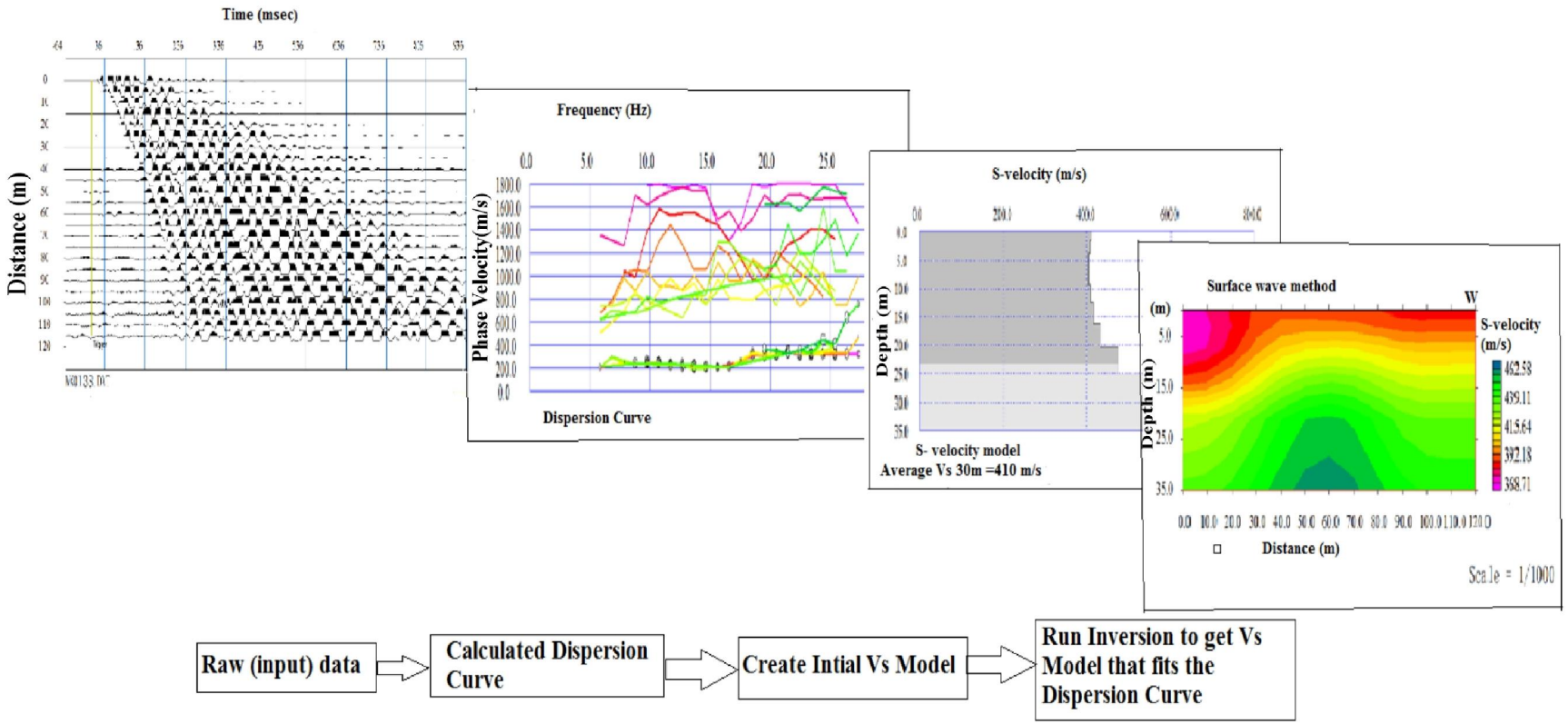

Figure 4.7 General steps of the 2D Multichannel Analysis of Surface Waves (MASW)

CHPTER FIVE

5. RESULTS AND INTERPRETATIONS OF SEISMIC DATA

The estimation of soil amplification in the present study is based on shear wave velocities, site periods and amplification factors. A Vs30 map, site period and an amplification factor maps were produced for the upper 30 meter depth. Meaningful engineering seismological interpretations of all maps were done depending on the average shear wave velocity to a depth 30 meter. Borehole data helps to constrain the depth to the bedrock and to correlate these different units with the shear wave velocity model and tomographic seismic refraction model. The refraction tomography model helps to estimate the depth to the bed rock and the rock type. Attempts have also been made to determine the relationship of Vs30 with site periods and amplification factors.

5.1 Seismic Refraction Tomography

Seismic refraction tomography method is an effective method to obtain generalized subsurface information for characterization of the soil. In the present study fifteen seismic tomography sections were produced. Three of them have been selected for the interpretation as an example and the rest of them were put in the appendix I. In the study area only one borehole is available. From these information, the bedrock structure, the p wave velocity distribution and depth underlying layers can be obtained. In general based on the seismic tomography section the area is characterized by three main layers. The top layer with velocity less than 500m/s is predominantly made up of top soils. This layer extends to average depth of 15 meters. From the average velocity values and borehole data this layer is suggested to be clay and lacustrine deposits.

As the depth increases the velocity slightly increases this is occurred when the p wave encounters different medium. The velocity ranges in the second layer from 500m/s to 800m/s which indicates by unwelded tuff. This layer is found at an average depth of 8 to 18meters.The 3rd layer has velocity greater than 1000m/s and it is located at depth greater than 18m. From the calculated velocity and borehole information, this layer is suggested to be competent tuff unit.

Site 4 and the borehole are located in the north western part of the area. As it is seen in (Fig. 5.1) the result of seismic tomographic section and the borehole data are correlated. The p wave velocity value is very low less than 400m/s. These p wave velocity range are response of clay and sediment deposits. The thickness of the layer varies from10 to18m.

The second layer p-wave velocity values range from 400m/s to 1000m/s. This velocity values correspond to the weathered and fractured tuff. The morphology of this layer is somehow undulating, due to this reason the thickness of this layer is varying from 4m in the center to 10m in both ends. The third layer with p wave velocity value greater than 1000m/s is the response of the bedrock which is much more welded and compacted tuff. The depth to the bedrock is varying from 18m to 25m.

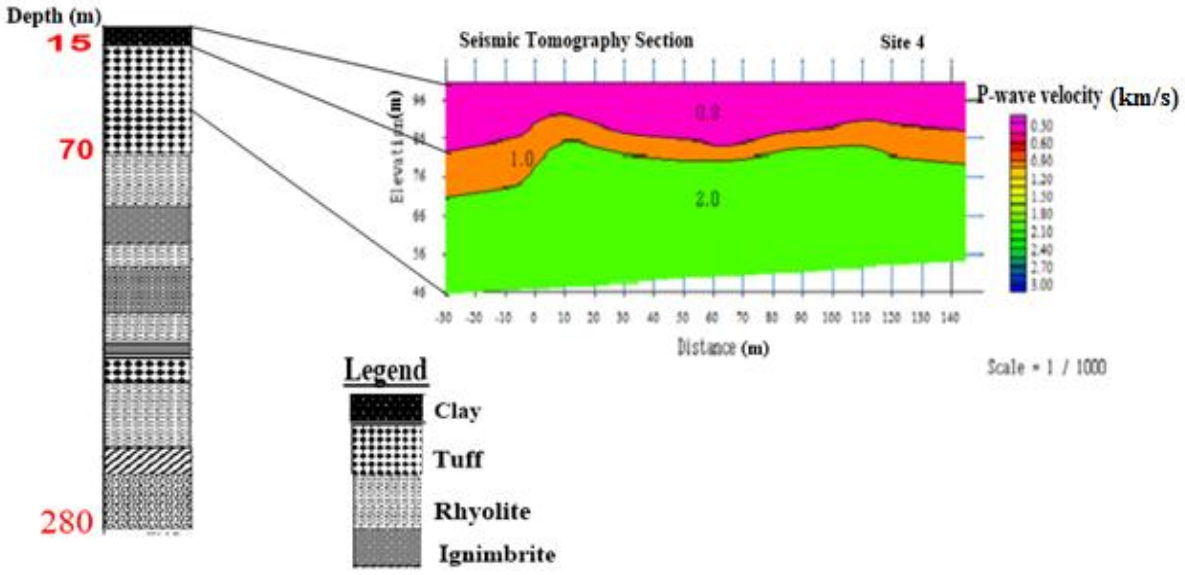

Figure 5.1 Interpretation of site 4 in relation to the borehole data

At site 12 the bedrock is exposed on the surface at a distance from 90 to 145m within the spread cable. The Plotrefa software(program) produced the tomographic model of this at 8 iterations resulting root mean square error (RMS error) of 1.98msec. The remaining part of this site (from -30 to 90m) constrains three layers which are similar to site 4. The only difference is the existence of the bedrock exposure on the surface in site 12 due to the fault.

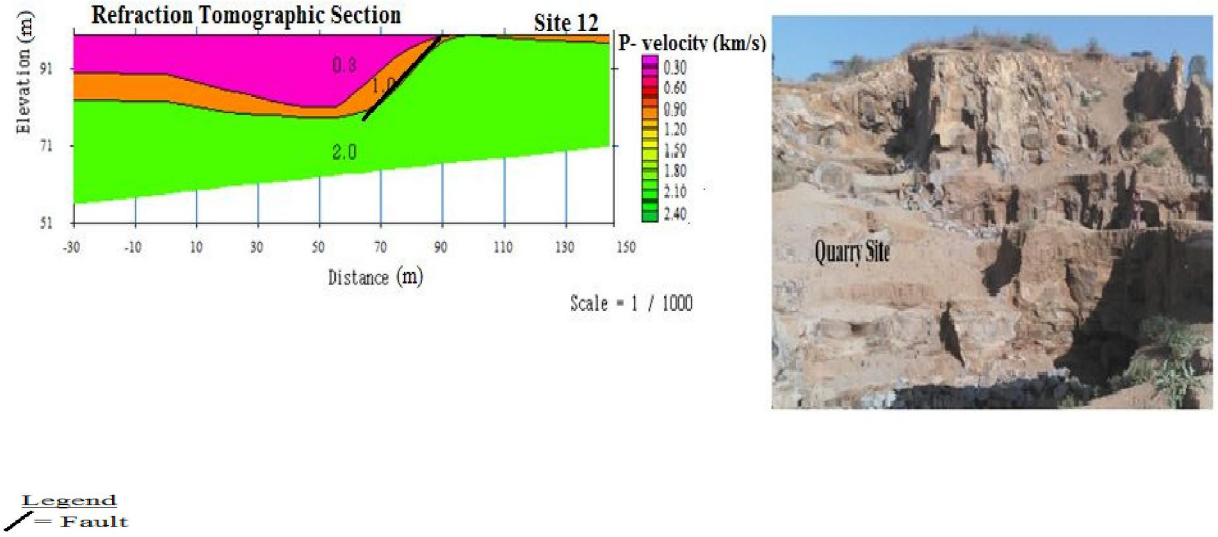

Figure 5.2 Interpretation of site 12 in relation to bedrock exposure due to fault structure

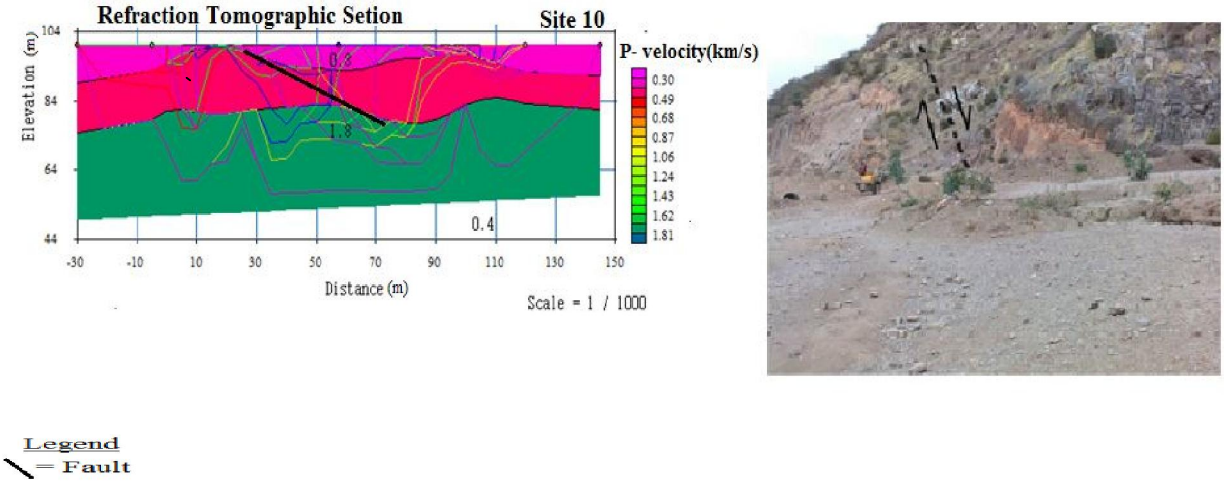

Figure 5.3 Correlation between seismic tomography section and fault structure at site 10

This correlation shows the existence of weak zone in the area. As it is observed in (fig. 5.3) geologically it is exposed in the surface and from seismic tomographic section results there is a transition of p-wave velocity value from 500 m/s to1800 m/s. Therefore, the transition of p-wave velocity value indicates the existence of structure.

5.2 Surface Wave Tomography

5.2.1 2D shear wave velocity distributions

The average shear wave velocity down to 30 m depth, which is obtained from the MASW technique, plays a critical role in evaluating the site response of the upper 30 m depth. The distribution of the obtained values of Vs through the studied area demonstrates site classes of C and D, according to the NEHRP (National Earthquake Hazard Reduction Program) and IBC (International Building Code) standards.

The 2D tomographic inversion results for all the sites are given in Figure below. The models site 3,4,7,9,12,and 18 has been classified under class D. Since their shear wave velocity value is less than 360m/s. The remaining models are classified under site class C. while the average shear wave velocity for the sites is greater than 360m/s. The survey in sites 1and 9 were oriented in east west direction. While in all the other sites the survey orientation north east direction.

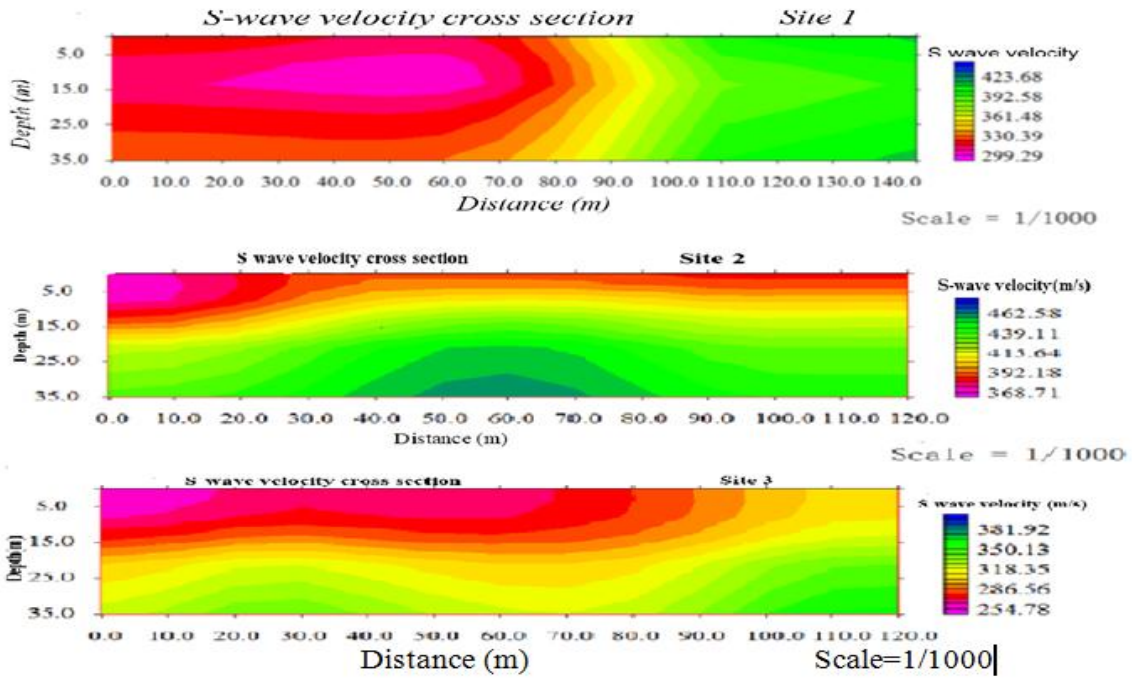

Figure5.3 Shows S-wave cross section of sites 1,2 and 3

Site 1 is located in south west part of the study area. As it is observed from the 2D model, the shear wave velocity increases from east to west of the survey. The average shear wave velocity of the upper 30m depth of the site is 382.6m/s. According to the NEHRP and IBC standards the Vs_{30} value of this site is classified as C class.

In sites 2and 3 the shear wave velocity increases with depth. These sites were located in the north west of the area. The survey lines were oriented north-south. The average shear wave velocities of the top 30m values are 410m/s and 275.4m/s for sites 2 and 3, respectively. Site 2 was classified under site class C while, site 3 was classified as D class.

Sites 4, 5 and 6 were located in the central north part of the study area. The orientation of the survey lines in these sites was in the north east direction. The shear wave velocity increases from north to east in site 4 and in sites 5 and 6 the shear wave velocity increases with depth. The average shear wave velocity of top 30m depth for site 4 is 326.3m/s and for sites 5 and 6 are 360.7m/s and 363.1m/s respectively. Based on these values site 4 is classified under site class D and while, 5 and 6 are classified under site class C.

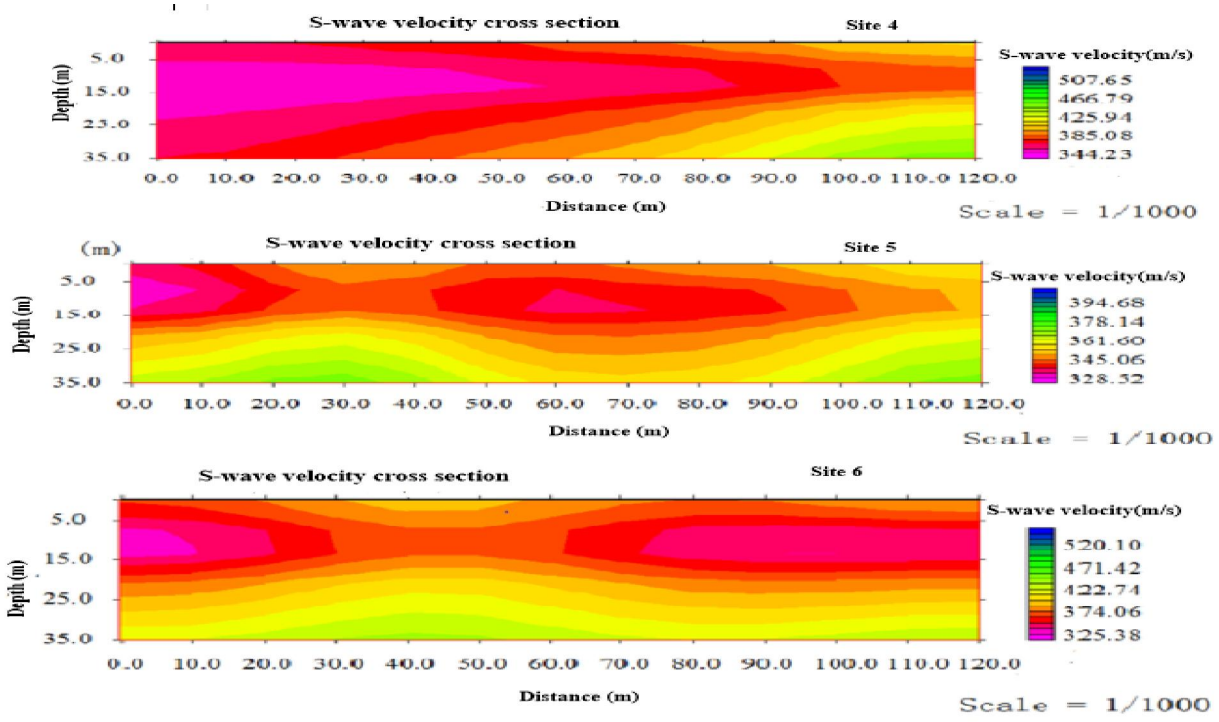

Figure5.4 Shows S-wave cross section of sites 4,5 and 6

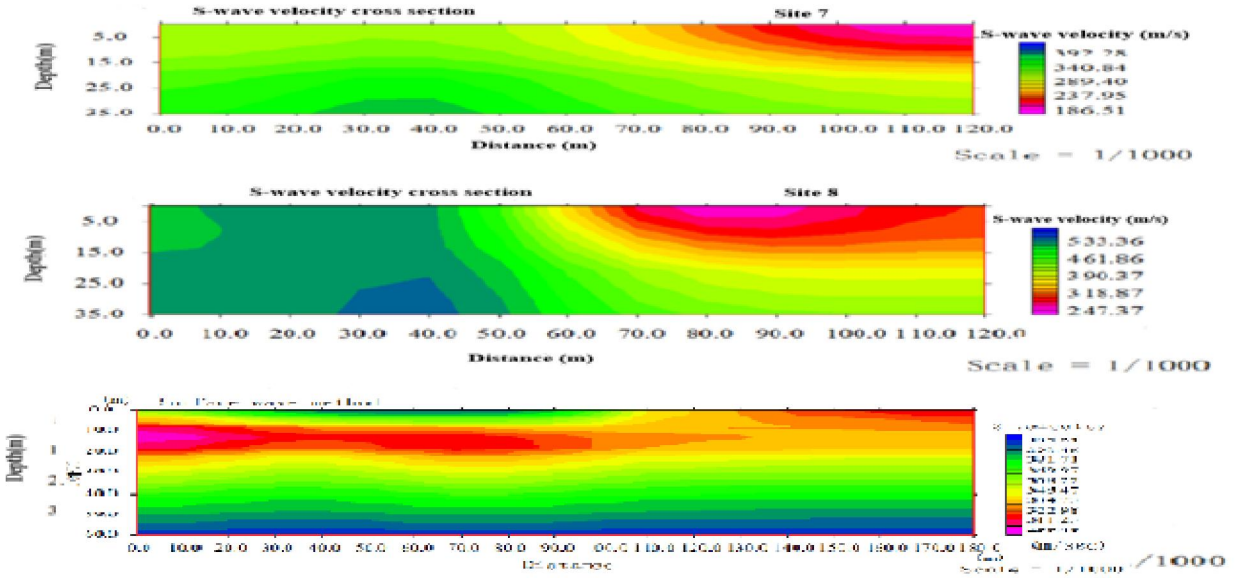

Figure 5.5 Shows S-wave cross section of sites 7,8 and 9

Sites 7, 8 and 9 were located in the central west part of the study area. The survey line orientation of sites 7and 8 was in the north east direction and in the east-west direction for site 9. The shear wave velocity decreases from north to south in sites 7 and 8 as it is seen in the above models. But it is almost constant in site 9 throughout the survey line. The average shear wave velocities of the upper 30m for site 7 is 287.6m/s, site 8 is 519.5m/s and site 9 is 271.8m/s. Sites 7and 9 are classified under site class D and site 8 is classified under site class C.

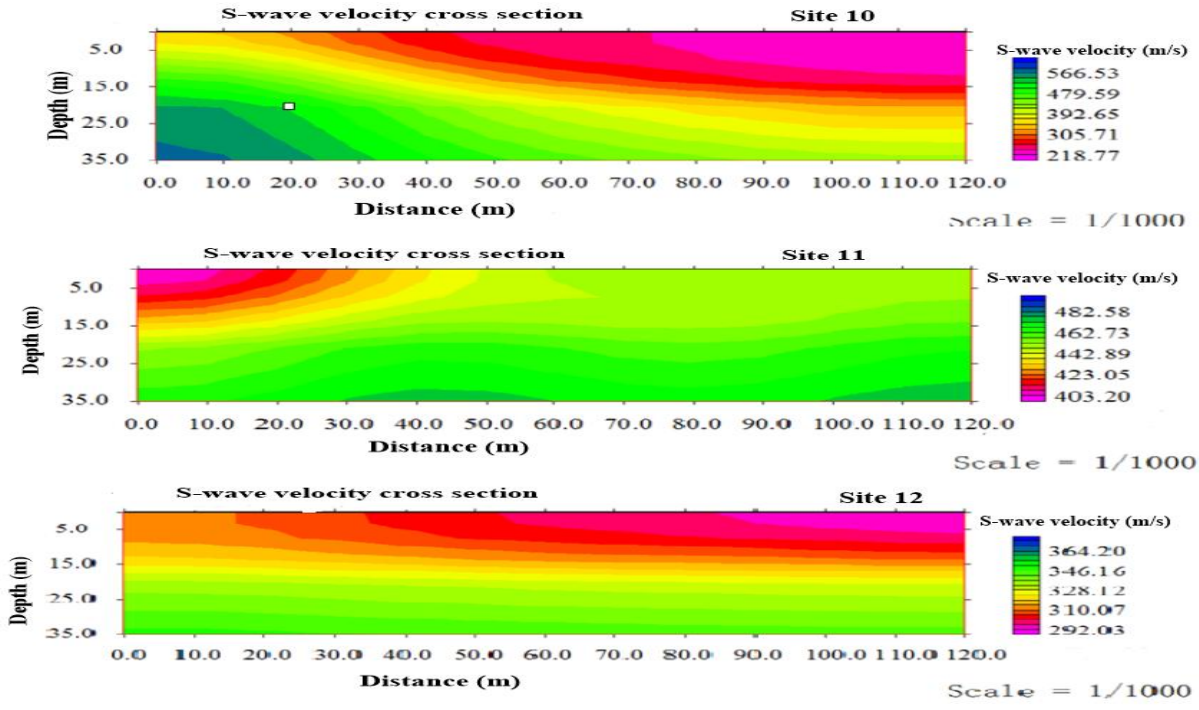

Figure 5.6 Shows S-wave cross section of sites 10, 11 and 12

Site 10, 11 and 12 were situated in the central west part of the area. The orientation of the survey lines in these sites were north-east. As it is observed in Figure 5.6 , the shear wave velocities in sites 10 and 12 decrease from north to east within the survey line but in site 11 the shear wave velocity is in the reverse way. The average shear wave velocity of the top 30m for site 10 is 406.6m/s, for site 11 it is 371m/s and for site 12 it 310m. Site 10 and 11 are classified as site class C whereas site 12 is in class D.

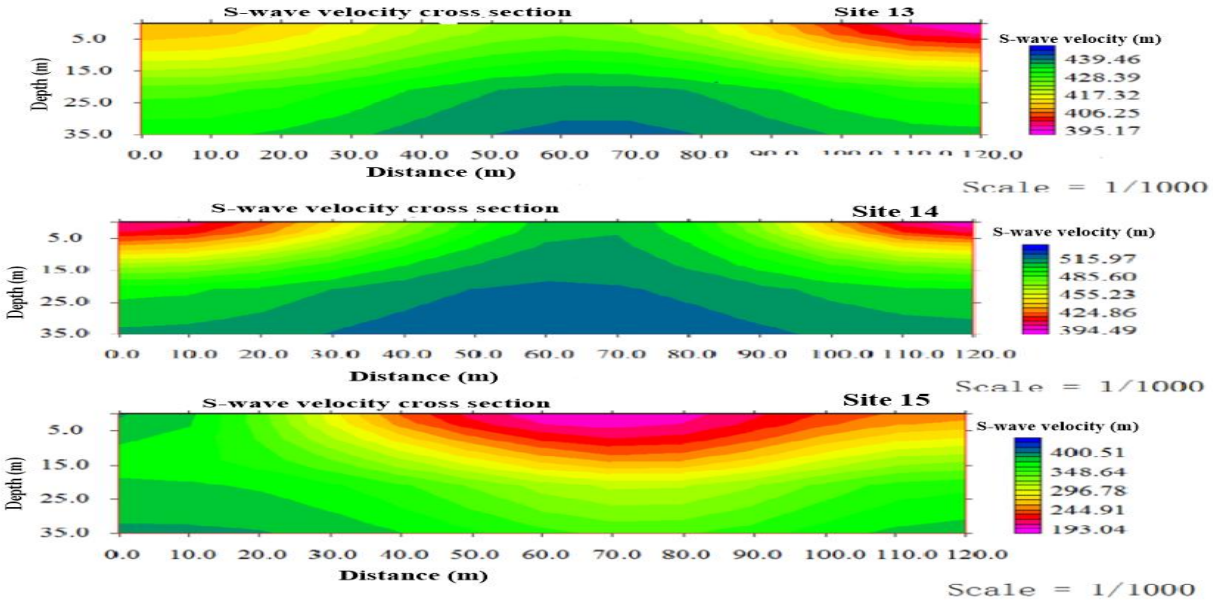

Figure 5.7 Shows S-wave cross section of sites 13,14 and 15

Sites 13, 14 and 15 were placed in the central southern portion of the area. The survey lines were oriented from northeast to southwest. The shear wave velocities in these sites increase with depth. The average shear wave velocities of the upper 30m depth for these site are 481m/s, 400.8m/s and 472.9m/s respectively. All sites in these figure are classified under site class C.

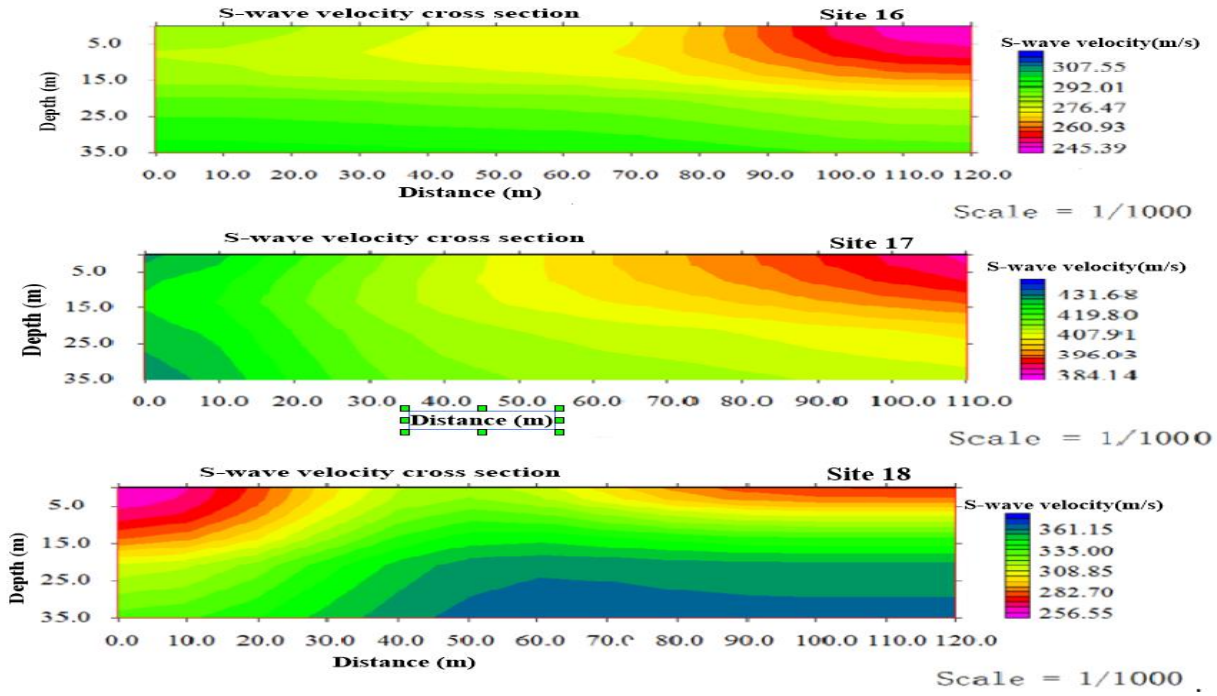

Figure 5.8 Shows S-wave cross section of sites 16, 17 and 18

Sites 16 and 17 were located in the central east but site 18 was located in the easternmost corner of the area. The orientation of the survey lines in is north east direction. The shear wave velocity decreases in site 16 and 17 but increases in site 18. The average shear wave velocities of the top 30m depth of the sites are 435.9m/s, 419.4m/s and 312.7m/s respectively. Site 16 and 17 belong to site class C and site 18 belongs to site class D.

5.2.1 The shear velocity distribution

The elastic properties of near surface materials and their effect on seismic wave propagation is very crucial in earthquake engineering, in environmental and in Earth Sciences. The increasing of amplitude in soft sediments is one of the most important factor responsible for the amplification of an earthquake motion (Maheswari et al ,2010). For soil amplification and site response studies, the 30 meter average shear wave is considered sufficient (Anbazhagan and Sitharam,2008). Vs_{30} is obtained by (Kanli, 2006):

$$Vs_{30} = \frac{30}{\sum_{i=1}^{N} \frac{d_i}{v_i}} \qquad (5.1)$$

Where d_i and v_i represent i^{th} layer's thickness and velocity.

The shear wave velocity distribution down to a depth of 30 meter is shown in Fig. 5.9. It consists of three different velocity zones. The northeastern and central western parts of the area - dark to light blue colored zones - are characterized by low shear wave velocity values of less than 340 m/s. This indicates the area is covered by soft clay and loose unsaturated sandy lacustrine deposits. The blue colored northernmost part of the area is simply the result of the minimum curvature interpolation artifacts from the software Surfer since data is lacking in that part.

The bulk of the area, in the central, northwest and southwest parts, shown in green is characterized by medium shear wave velocities ranging between 340m/s and 440m/s. From geological map and Vs value the stratigraphy consists of Clay, sand clay, weathered and fractured ignimbrite and rhyolite layers. The central and southern parts of the area (yellow to reddish color) are characterized by high shear velocity values of greater than 440m/s. This is characterized by shallow bed rock overlain by slightly compacted clay, saturated sand and weathered basalt.

The calculated average shear wave velocities are grouped according to the NEHRP site classes and a map has been generated using Surfer Software Package. Based on this the study area is considered to consist of two classes for seismic local site effects. These are C and D classes. With most parts of the study area falling in site class C (Vs_{30} > 360m/s). The remaining part falls to site class D (Vs_{30} < 360m/s). The map in Fig.5.1 shows the average shear wave velocity distribution to a depth of 30m.

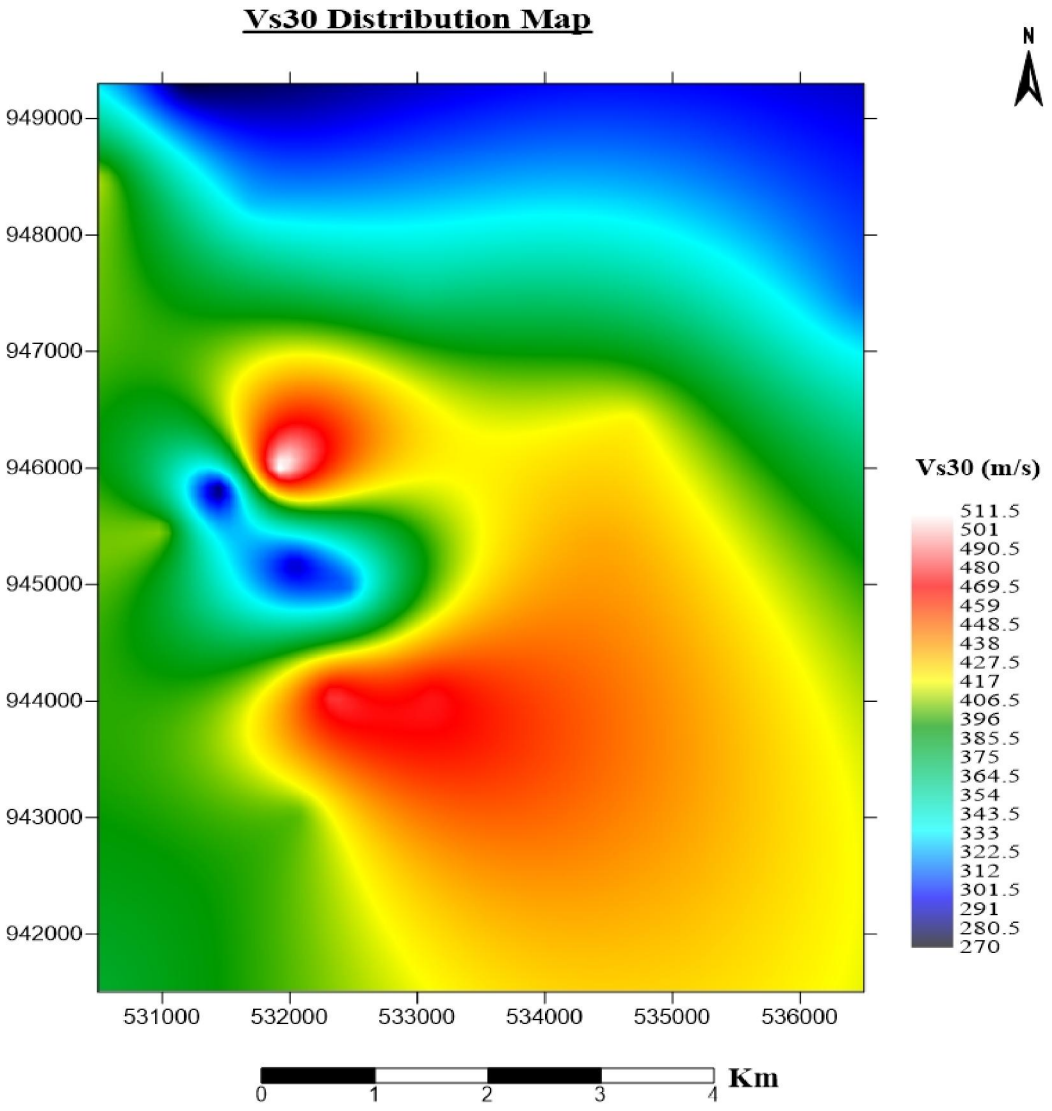

Figure 5.9 Vs_{30} Distribution Map

5.2.2 Site Period

The characteristic site period (or site dominant frequency f_s) which depends on the thickness (H) and shear wave velocity (Vs) of the soil provides a very useful indication of the period of vibration at which the most significant amplification can be expected (Dabbeek, 2011). According to Rathje and Navidi (2013) site period is calculated using the following expression:

$$T_s = \frac{4 \cdot H}{\bar{V}_s} \qquad (5.2)$$

Where H is the soil thickness and Vs is the average shear wave velocity of the soil. Applying eq. 5.2 to the top 30m, we have:

$$T_{30} = \frac{4 \cdot (30\ \mathrm{m})}{V_{s30}} \qquad (5.3)$$

Since the site period is inversely proportional to the average shear wave velocity, T_{30} decreases as Vs_{30} increases. Hence, stiff layers have shorter periods. The calculated site periods for the area are shown in Table 5.1 and the site periods are plotted against shear wave velocities in Fig. 5.10. They show an inverse relationship.

Table 5.1 T_{30} values for each Vs_{30}

Vs30 (m/s)	T30 (Sec)	Vs30 (m/s)	T30 (Sec)
382.6	0.314	406.6	0.297
410	0.293	371	0.323
275.4	0.436	310	0.387
326.3	0.368	481	0.249
360.7	0.333	400.8	0.299
363.1	0.33	472.9	0.254
287.6	0.417	435.9	0.275
519.5	0.231	419.4	0.286
271.8	0.442	312.7	0.384

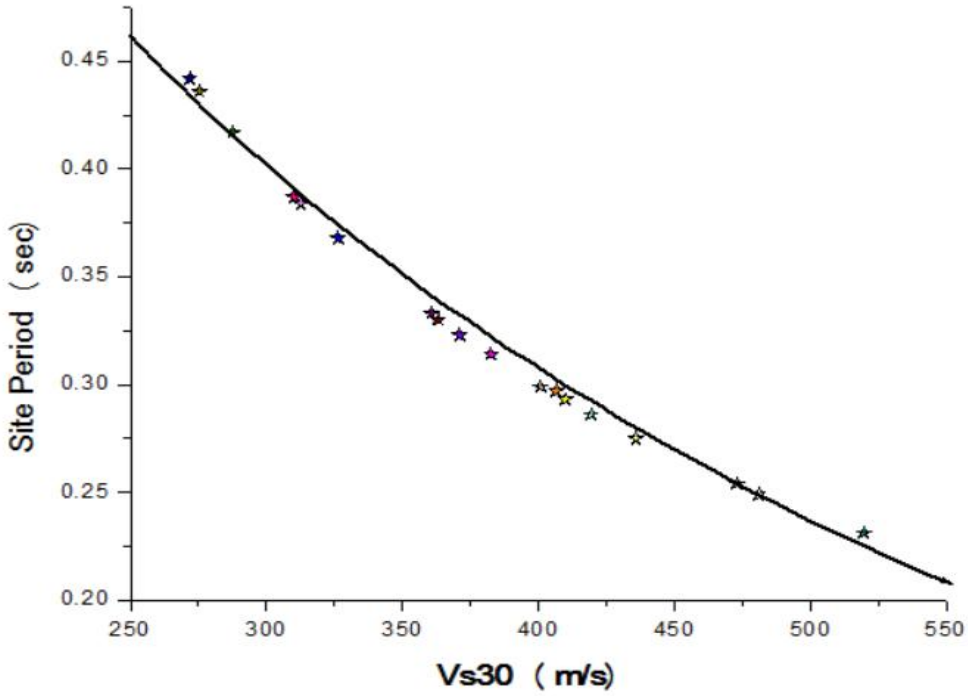

Figure 5.10 Site period versus Vs30 graph

The site period map for the area is presented in Fig. 5.11. This map indicates the north, northeastern and central west parts (reddish color) are characterized by high site period values ranging between 0.35s and 0.45s with frequency (2.22 - 2.86 Hz). The central, northwestern and southwestern parts shown in green indicate medium site period values. The range of this value is between 0.29s and 0.34s with frequency (2.94 - 3.45 Hz). The third category is the light to dark blue colored part exposed in the central and southeastern part of the area where the site period is low or less than 0.27s and the frequency is greater than 3.65 Hz.

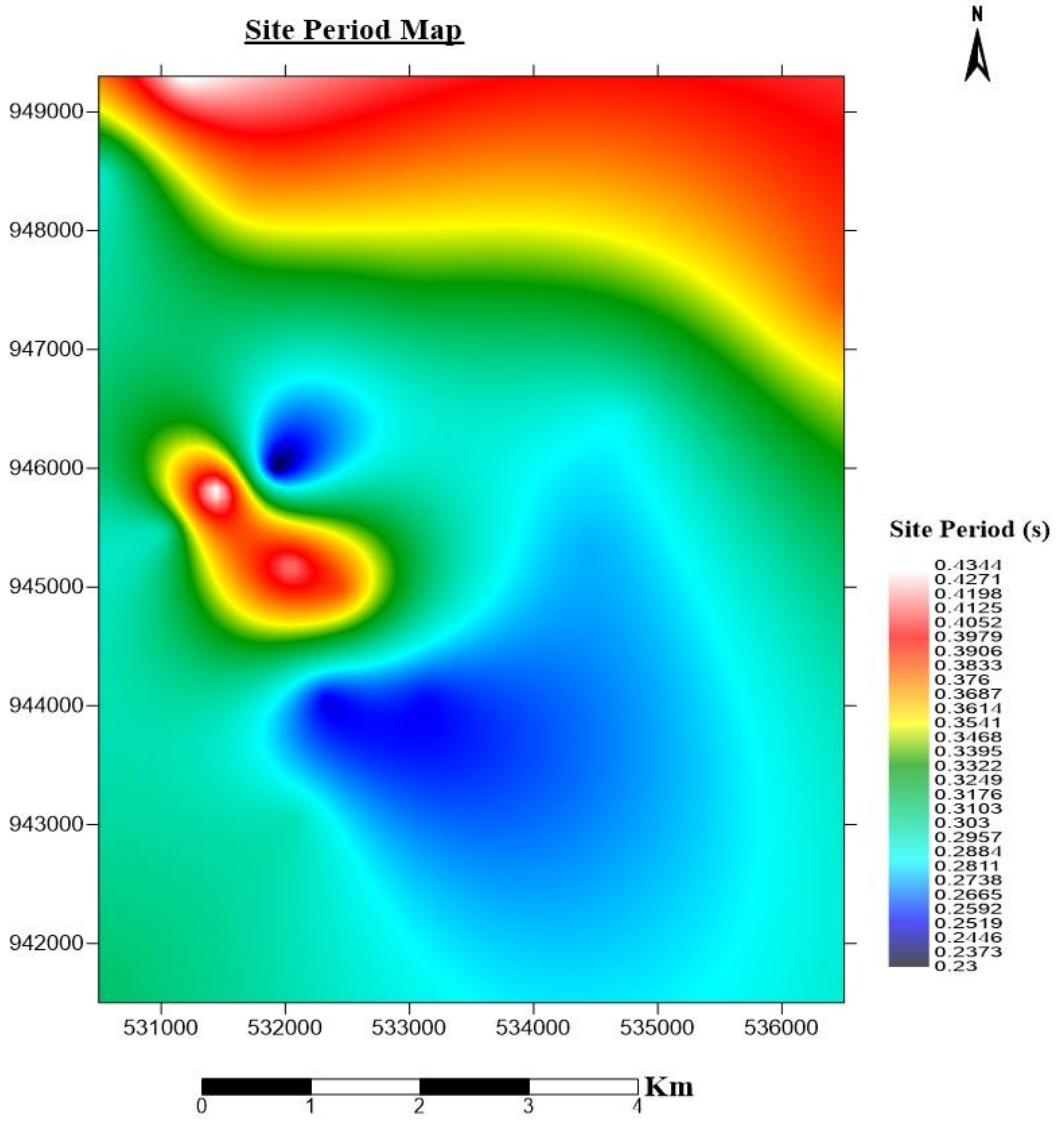

Figure 5.11 Site Period Map of the Study Area

5.2.3 Amplification Factor

Amplification factor is a parameter that is directly related to the seismic hazard of the area. Originally maximum amplification factors were obtained within the acceleration, velocity and displacement controlled regions as they are usually presented in such a format in codes and guidelines. The results showed that there was no real trend with depth or shear wave velocity of the site when the amplification factors were obtained in such a manner. This is because while the magnitude of the amplification factor is highly dependent on the shear wave velocity, the location of the amplification is highly dependent on the site's period.

According to Ishihara (2015) the amplification factor for specific period range is a function of Vs30. For periods greater than 0.5sec the amplification factors are not very sensitive to period but are much greater than the short period amplification factor for the period less than 0.5sec. This book adopt two sets of amplification factors; one set for short periods (T < 0.5sec) and another set for long periods (T > 0.5).

In the present study the range of site period belongs to the short periods (T< 0.5). The period dependent amplification factor are calculated using the following formula:

$AF = (997m/s/V)^{0.36}$ (5.4)

Where V is the average shear wave velocity to 30m depth measured in m/s

Based on this relation, the amplification factors for the study are shown in Table 5.2.

Table 5.2 Amplification Factor values for each Vs_{30}

Vs30(m/s)	Amplification Factor	Vs30(m/s)	Amplification Factor
382.6	1.4	406.6	1.38
410	1.38	371	1.43
275.4	1.6	310	1.52
326.3	1.5	481	1.3
360.7	1.44	400.8	1.39
363.1	1.438	472.9	1.31
287.6	1.56	435.9	1.35
519.5	1.26	419.4	1.37
271.8	1.6	312.7	1.52

As it is seen in the graph below there is a inversely proportionality relation between amplification factors and shear wave velocity values. That means as the shear wave velocity increases the value of amplification factor also decreases and vice versa.

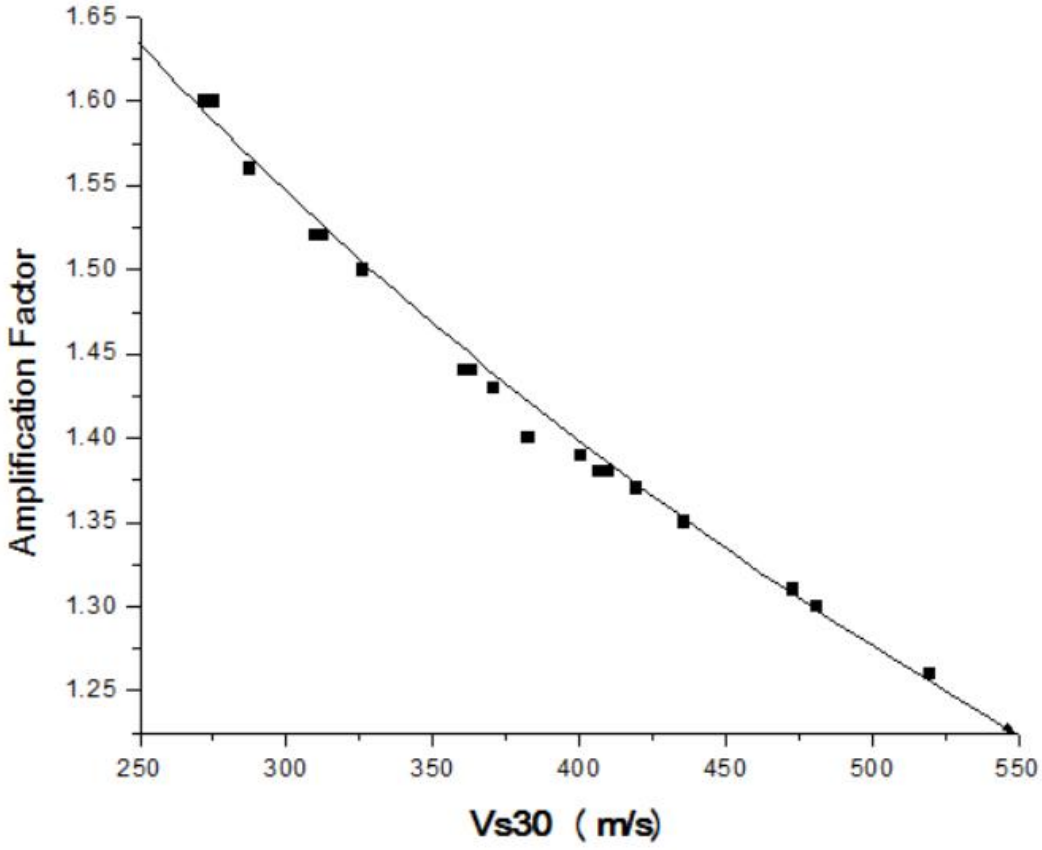

Figure 5.12 Vs30 versus amplification Factor graph

The calculated amplification factor in this study ranges from 1.26 to 1.6. The quantitative amplification factors were obtained and these results were used to prepare the amplification factor map. The value of amplification factor for the study area is larger where the value of Vs30 is low in the north, northeast and central west with a color range red to yellowish. Lower amplification factor values were also found where the values of Vs30 is higher in most parts of the map shown by blue color which is observed in the central and south west.

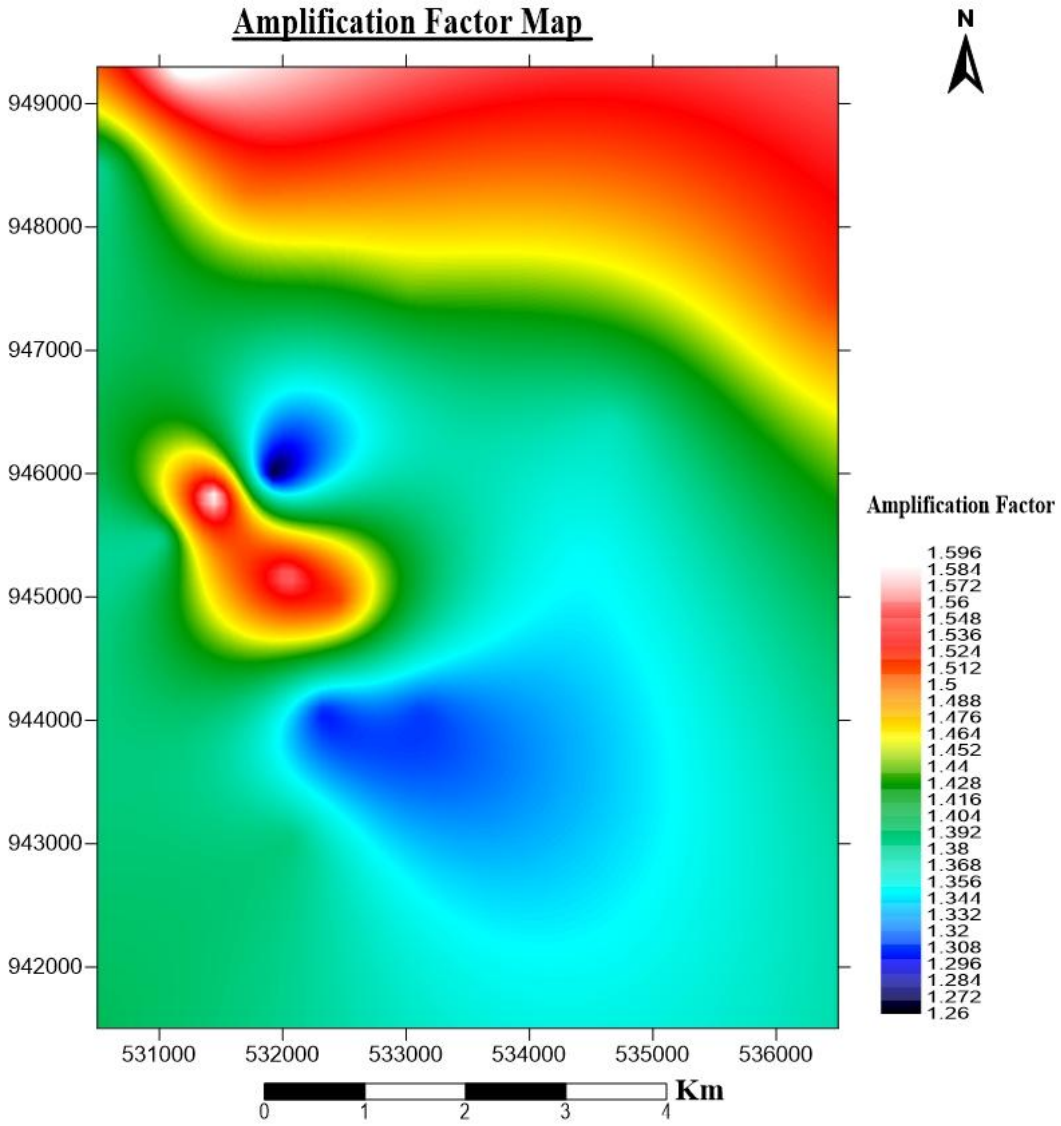

Figure 5.13 Amplification Factor Map of the study area

5.2.4 Variability in Amplification Factors

Amplification factor varies as the value of Vs30 varies. Figure 5.14 plots amplification factor versus period for all sites for each of the Vs30 values. The amplification factors for a given VS30 are not constant and show significant scatter. The amount of scatter (i.e. variability) varies with VS30 and period.

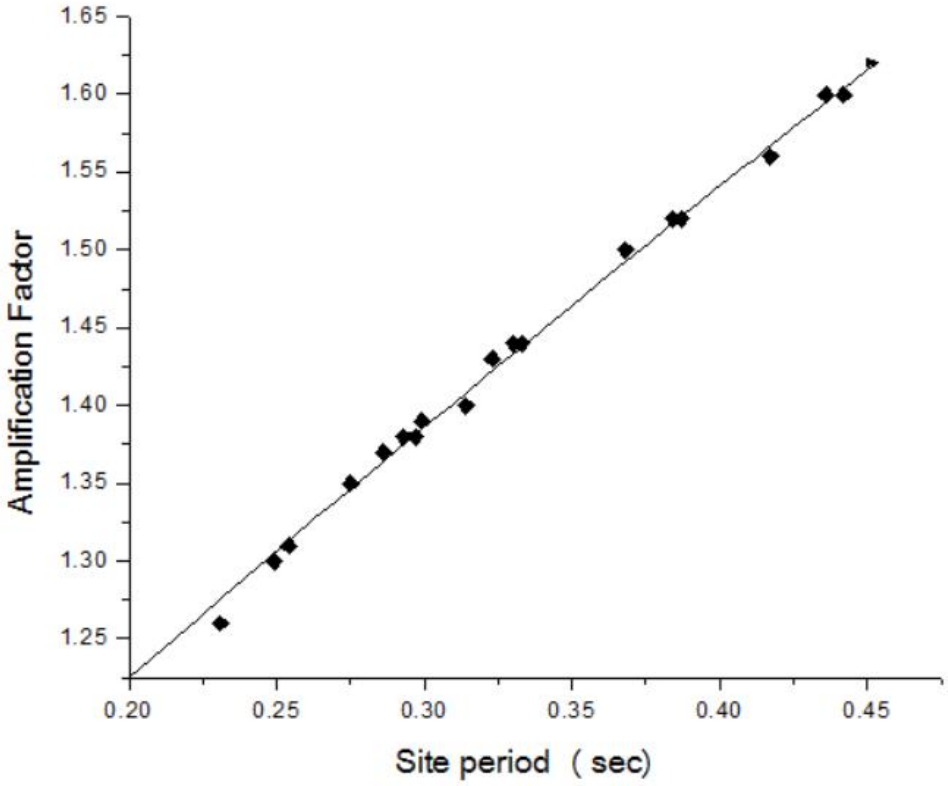

Figure 5.14 Site period versus amplification factor graph

CHPTER SIX

6. CONCLUSION AND RECOMMENDATION

6.1 Conclusion

Soil amplification studies involving seismic methods (both P-wave and S-wave studies) were carried out in some selected parts of Adama town. Most part of the area is characterized by flat topography that is surrounded by ridges and it is covered by lacustrine deposits.

Both seismic refraction and surface wave studies suggest that the soil thickness is considerably large exceeding 20 m. Seismic refraction analysis reveal that the study area consists of three layers depending on their p-wave velocity. Correlations between geology and seismic tomographic section have been made to identify presence of different geological structure. The uppermost layer with velocity less than 500m/s is predominantly made up of top soils of clay and lacustrine sediments. It extends to an average depth of 15 meters. The second layer with p-wave velocity value ranging from 500m/s to 1000m/s corresponds to be unwelded tuff. The 3rd layer has velocity greater than 1000m/s and a depth greater than 18m. From the calculated velocity and borehole information, this layer may be competent tuff unit. The study confirms the existence of fault structures and thick soil overlying the bedrock. The thick soil amplifies the magnitude of an earthquake and it enhances seismic hazard.

Multichannel analyses of surface waves reveal the average shear wave velocity in the upper 30m is in the range 270 - 550m/s. According to the NEHRP the soil can be categorized into class C and D, with the major part of the study area falling into site class C.

Soil amplification of a site is expressed in terms of amplification factor. The calculated value of amplification factor for the site ranges from 1.26 to 1.6. The higher values of the amplification factors are located in the central west and northern portions and in these parts the higher amplification factor shows high amplification potential and high seismic hazard. Lower values of amplification factor are found in central and towards south central parts of the study area. In these sites the lower amplification factor indicates low amplification potential of the soil and relatively low seismic hazard. The damage due to seismic hazard is much higher on the unconsolidated soils than on solid rocks.

Generally, from both results it was seen that thick soil deposit overlies the bedrock found about below 20m depth. Therefore, soil of the area amplifies the magnitude of an earthquake and it enhances seismic hazard.

6.2 Recommendations

Since Adama is one the fastest growing cities in the country huge construction works are ongoing. In addition, the growth of trade and commerce is very high in the city. Based on the present study, the following recommendations are made in relation to the soil response to seismic hazard:

- To mitigate seismic hazard due to local soil condition, it is necessary to prepare detailed seismic microzonation map of the area.
- The Building Code of the country should be revised to include site-specific conditions based on much more refined seismic microzonation map.
- It is recommended to adopt regulations that require geologic and seismic site investigations before development proposals can be approved.
- There should be a trend of construction towards low rise buildings with reinforcement of the existing ones to resist earthquake damage.
- It is also recommended that the local population be made aware of the risks and know how to act during an earthquake.

REFERENCES

Agostini, A., Bonini, M., Corti, G., Sani, F. and Manetti, P. (2011). Distribution of quaternary deformation in the central Main Ethiopian Rift, East Africa, *Tectonics*, *30*(4).

Aki, K. and Richards, P. G. (1980). Quantitative Seismology: Theory and Methods Freeman, *New York*.

Alula Damte, Boccaletti, M., Getaneh Assefa, Mazzuoli R. and Tortorici, L. (1992). Geological Map of the Nazareth-Dera Region, 1:50,000 Scales, Consiglio Nazionale Delle Ricerche, Italy.

Amaha Atnafu, Cuffaro, M. and Doglioni, C. (2014). Left-lateral transtension along the Ethiopian Rift and constrains on the mantle-reference plate motions, *Tectonophysics*, ***632***: 21-31.

Anbazhagan, P. and Sitharam, T. G. (2008). Site characterization and site response studies using shear wave velocity, *Journal of Seismology and Earthquake Engineering*, ***10***(2): 53.

Anbazhagan, P., Thingbaijam, K. K. S., Nath, S. K., Kumar, J. N. and Sitharam, T. G. (2010), Multi-criteria seismic hazard evaluation for Bangalore city, India, *Journal of Asian Earth Sciences*, ***38***(5): 186-198.

Arif, A., Saad, M. and Abdulaziz, N. (2012). Time independent seismic hazard analysis of the afar depression, *Academic Journals*, **7**(14): 1494-1500.

Atalay Ayele (1995). Earthquake Catalogue of the Horn of Africa for the period 1960-93, Seism. Dept., Uppsala Univ. Rept. **3**(95): 1-32.

Atalay Ayele and Kulhanek, O. (1997). Spatial and Temporal variation of seismicity in the Horn of Africa 1960-1993, RASGJI **130**: 805-810.

Atalay Ayele, Stuart, G., Bastow, I. and Keir, D. (2007). The August 2002 earthquake sequence in north Afar: Insights into the neotectonics of the Danakil microplate, *Journal of African Earth Sciences*, ***48***(2): 70-79.

Azwin, I. N., Saad, R. and Nordiana, M. (2013). Applying the Seismic Refraction Tomography for Site Characterization. *APCBEE Procedia*, ***5***: 227-231.

Bigazzi, B., Bonadonna, F. P., Di Paola, G. M. and Giuliani, A. (1993). K-Ar and fission track ages of the last volcano tectonic phase in the Ethiopian Rift Valley (Tullu Moye area), *Geology and mineral resources of Somalia and surrounding regions, Istituto Agronomico Oltremare, Firenze, Relazioni Monografie*, ***113***: 311-322.

Boccaletti, M., Bonini, M., Mazzuoli, R.,Bekele Abebe, Piccardi, L. and Tortorici, L. (1998). Quaternary oblique extensional tectonics in the Ethiopian Rift (Horn of Africa), *Tectonophysics*, ***287***(1): 97-116.

Boccaletti, M., Bonini, M., Mazzuoli, R. and Trua, T. (1999). Pliocene-Quaternary volcanism and faulting in the northern Main Ethiopian Rift (with two geological maps at scale 1: 50,000), *Acta vulcanologica*, ***11***: 83-98.

Boccaletti, M., Getaneh Asefa and Tortorici, L. (1992). The Main Ethiopian Rift: an example of oblique rifting, In *Annales Tectonicae* **6**(1): 20-25.

Borcherdt, R. D. (1994). Estimates of site-dependent response spectra for design (methodology and justification), *Earthquake spectra*, ***10***(4): 617-653.

Dabbeek, J. A. and ESSEC Team An-Najah National University (2011). Assessment of Seismic Site Effect for Rawabi First Palestinian Planned City, Nablus, Palestine Geneva.

Ellen, M. R. and Sara, N. (2013). Identification of Site Parameters that Improve Predictions of Site Amplification, Pacific Earthquake Engineering Research Center, 28pp.

Fekadu Kebede (1997). Hazard Maps of Spectral Response Acceleration for Ethiopia, In *Proceedings of the Second Symposium of the Ethiopian Association of Seismology and Earthquake Engineering (EASEE), Addis Ababa, Ethiopia*.

Fekadu Kebede and Laike Mariam Asfaw(1996). Seismic hazard assessment for Ethiopia and the neighboring countries, *Sinet*, ***19***(1): 15-50.

Getahun Kebede (1987). Hydrogeology of Nazreth area, NC 37-15, *Report to Ethiopian Institute of Geological Surveys, Ministry of Mines and Energy, 106pp*.

Green, R. A., Olson, S. M., Cox, B. R., Rix, G. J., Rathje, E., Bachhuber, J. and Martin, N. (2011). Geotechnical aspects of failures at Port-au-Prince seaport during the 12 January 2010 Haiti earthquake, *Earthquake Spectra*, ***27*****(**1): 43-65.

Gouin, P. (1979). *Earthquake history of Ethiopia and the Horn of Africa*.

Gupta, I. D. (2002). The state of the art in seismic hazard analysis, *ISET Journal of Earthquake Technology*, ***39***(4): 311-346.

Gupta, I. D. (2007). Probabilistic seismic hazard analysis method for mapping of spectral amplitudes and other design-specific quantities to estimate the earthquake effects on man-made structures, *ISET J Earthq Tech*, ***44***(1): 127-167.

Habtom Gebremedhin (2006). Earthquake Hazard Assessment with the help of Remote Sensing and Gis Techniques (Doctoral dissertation, Addis Ababa University).

Ishihara, k.(2015). Perspectives on Earthquake Geotechnical Engineering*, Geotechnical, Geological and Earthquake Engineering,* 45pp.

Kanli, A. I., Tildy, P., Prónay, Z., Pınar, A. and Hermann, L. (2006). VS30 mapping and soil classification for seismic site effect evaluation in Dinar region, SW Turkey, *Geophysical Journal International*, ***165***(1): 223-235.

Kelly, D. (2006). Seismic Site Classification For Structural Engineers, *Structure*, *21*.

Kockar, M. K. (2006). *Engineering geological and geotechnical site characterization and determination of the seismic hazards of Upper Pliocene and Quaternary deposits situated towards the west of Ankara* (Doctoral dissertation, Middle East Technical University).

Kramer, S. L. (1996). *Geotechnical earthquake engineering*, Pearson Education India.

Kuo, C. H., Wen, K. L., Lin, C. M., Wen, S. and Huang, J. Y. (2015). Investigating Near Surface S-Wave Velocity Properties Using Ambient Noise in Southwestern Taiwan, *Terrestrial, Atmospheric and Oceanic Sciences*, *26*(2).

Messay Mulugeta (2010). Food security attainment role of urban agriculture: A case study of Adama town, Central Ethiopia, *Journal of Sustainable Development in Africa*, ***10***(30): 223-249.

Maheswari, R. U., Boominathan, A. and Dodagoudar, G. R. (2010). Seismic site classification and site period mapping of Chennai City using geophysical and geotechnical data, *Journal of Applied Geophysics*, ***72***(3): 152-168.

Maniatakis, C. A., Taflampas, I. M. and Spyrakos, C. C. (2008). Identification of near-fault earthquake record characteristics, In *the 14th world conference on earthquake engineering Beijing, China,* (pp. 12-17).

Mackenzie, G. D., Thybo, H., and Maguire, P. K. H. (2005). Crustal velocity structure across the Main Ethiopian Rift: results from two-dimensional wide-angle seismic modelling, *Geophysical Journal International*, ***162***(3): 994-1006.

Meyer, W., Pilger, A., Rosler, A. and Stets, J. (1975). Tectonic evolution of the northern part of the Main Ethiopian Rift in southern Ethiopia, In *Afar depression of Ethiopia* (pp. 352-362).

Michigan Tech (2004).UPSeis an educational site for building seismologists, (www.geo.mtu.edu/UPSeis/waves.html), accessed on march 24/2016.

Mohamed, A. M., El Ata, A. A., Azim, F. A. and Taha, M. A. (2013). Site-specific shear wave velocity investigation for geotechnical engineering applications using seismic refraction and 2D multi-channel analysis of surface waves, *NRIAG Journal of Astronomy and Geophysics*, ***2***(1): 88-101.

Mohamed, A. M., Hafiez, H. A. and Taha, M. A. (2013). Estimating the near-surface site response to mitigate earthquake disasters at the October 6th city, Egypt, using HVSR and seismic techniques, *NRIAG Journal of Astronomy and Geophysics*, ***2***(1): 146-165.

Mohr, P. (1967). The Ethiopian Rift System, Addis Ababa Geophysical observatory bulletin 11: 65.

Mohr, P. (1983). Volcanotectonic aspects of Ethiopian rift evolution, *Bull. Cent. Rech. Explor. Prod. Elf-Aquitaine*, ***7*:** 175-189.

Ozcep, F. and Ozcep, T. (2011). Geophysical analysis of the soils for civil (Geotechnical) engineering and urban planning purposes: Some case histories from Turkey, *International Journal of the Physical Sciences*, ***6***(5): 1169-1195.

Pei, D. (2007). *Modeling and inversion of dispersion curves of surface waves in shallow site investigations*, ProQuest.

Pekkan, E., Tun, M., Guney, Y. and Mutlu, S. (2015). Integrated seismic risk analysis using simple weighting method: the case of residential Eskisehir, Turkey, *Natural Hazards and Earth System Science*, ***15***(6), 1123-1133.

PMD, N. (2007). Seismic hazard analysis and zonation of Pakistan, Azad Jammu and Kashmir, *Pakistan Meteorological Department and Norway Report*.

Rathje ,E.M (2010). Site response program Strata available for free at,

(http://nees.org/resources/strata), accessed on December 12/2015.

Rathje, E. M. and Navidi, S. (2013). Pacific Earthquake Engineering Research Center.

Reynolds, J.M. (1997). An Introduction to Applied and Environmental Geophysics, John Wiley and Sons, Ltd, UK, 800 pp.

Samuel Kinde ,Samson Engeda, Asnake Kebede and Eyob Tessema (2011). Technical Notes: Notes and Proposed Guidelines on Updated Seismic Codes in Ethiopia-Implication for Large-Scale Infrastructures, *Zede Journal*, ***28***: 91-110.

Samuiel Kinde (2003). Issues in Seismic Zoning and Proposed Reconsiderations in Seismic Building Codes in Ethiopia University of California, Irvine.

Scawthorn, C. (2013). Pacific Earthquake Engineering Research Center.

Sitharam, T. G. and Anbazhagan, P. (2008). Seismic microzonation: principles, practices and experiments, *EJGE Special Volume Bouquet*, *8*.

Standard, E. B. C. (1995). Code of Standards for Seismic Loads, *Ministry of Works and Urban Development, Addis Ababa, Ethiopia*.

Strecker, M. and Blisniuk, P. (1992). Integration of East African Paleostress and Present-Day Stress Data Implications For Continental Stress Field Dynamics, *Journal of Geophysical Research*, ***97***(B8): 11-851.

Tigistu Haile, Tamiru Alemayehu and Gaetano, R. (2000) geophysical, geological and hydrogeological investigations of Boku thermal field, Nazareth, Ethiopia.

Tigistu Haile, Tamiru Alemayehu and Shimelis Fisseha (2004). Integrated geophysical investigations to study thermal zones at Boku volcanic Centre, Main Ethiopian Rift, *SINET: Ethiopian Journal of Science*, ***25***(2): 253-262.

Tilahun Mammo (2005). Site-specific ground motion simulation and seismic response analysis at the proposed bridge sites within the city of Addis Ababa, Ethiopia, *Engineering geology, **79***(3): 127-150.

US Army Corps of Engineers (1995). Geophysical Exploration for Engineering and Environmental Investigations, Engineering And Design , Washington, DC, U.S.A, 17pp.

Wald, D. J., Whirter, L., Thompson, E. and Hering, A. S. (2011). A new strategy for developing VS_{30} maps, In *Proc. 4th Int. Effects of Surface Geology on Seismic Motion Symp*.

Wolfenden, E., Ebinger, C., Gezahegn Yirgu, Deino, A. and Dereje Ayalew (2004). Evolution of the northern Main Ethiopian rift: birth of a triple junction, *Earth and Planetary Science Letters*, ***224***(1): 213-228.

Zone, E. A. R. (2003). Geophysical project in Ethiopia studies continental breakup, *Eos*, *84*(35).

Appendices

AppendixI: Sesmic Refraction Tomography of the sites

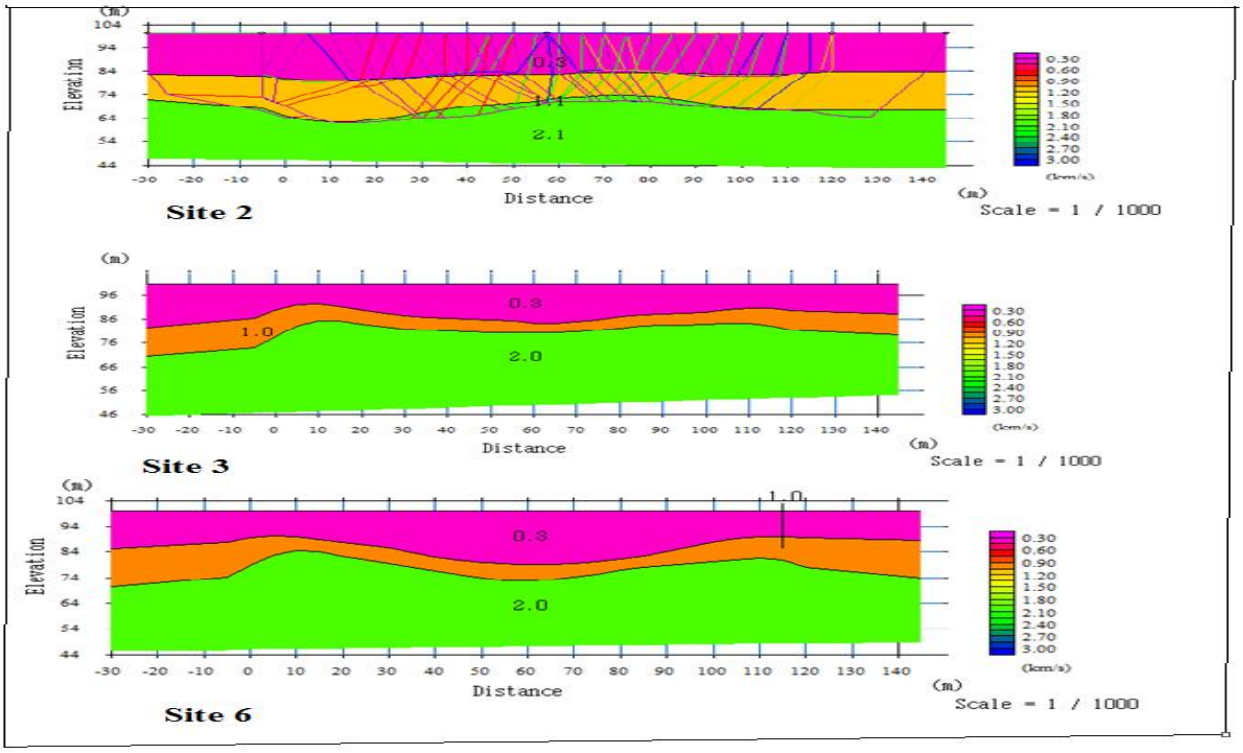

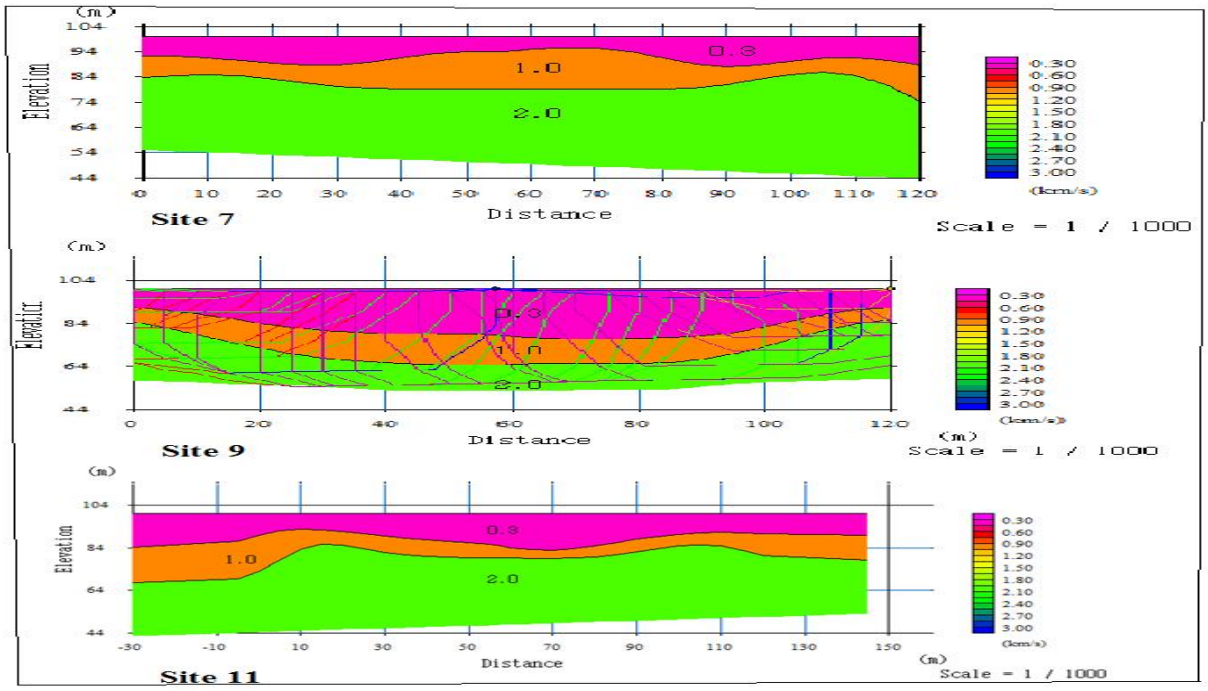
Site 7
Site 9
Site 11
Elevation
Distance
(m)
Scale = 1 / 1000
0.3
1.0
2.0
(km/s)

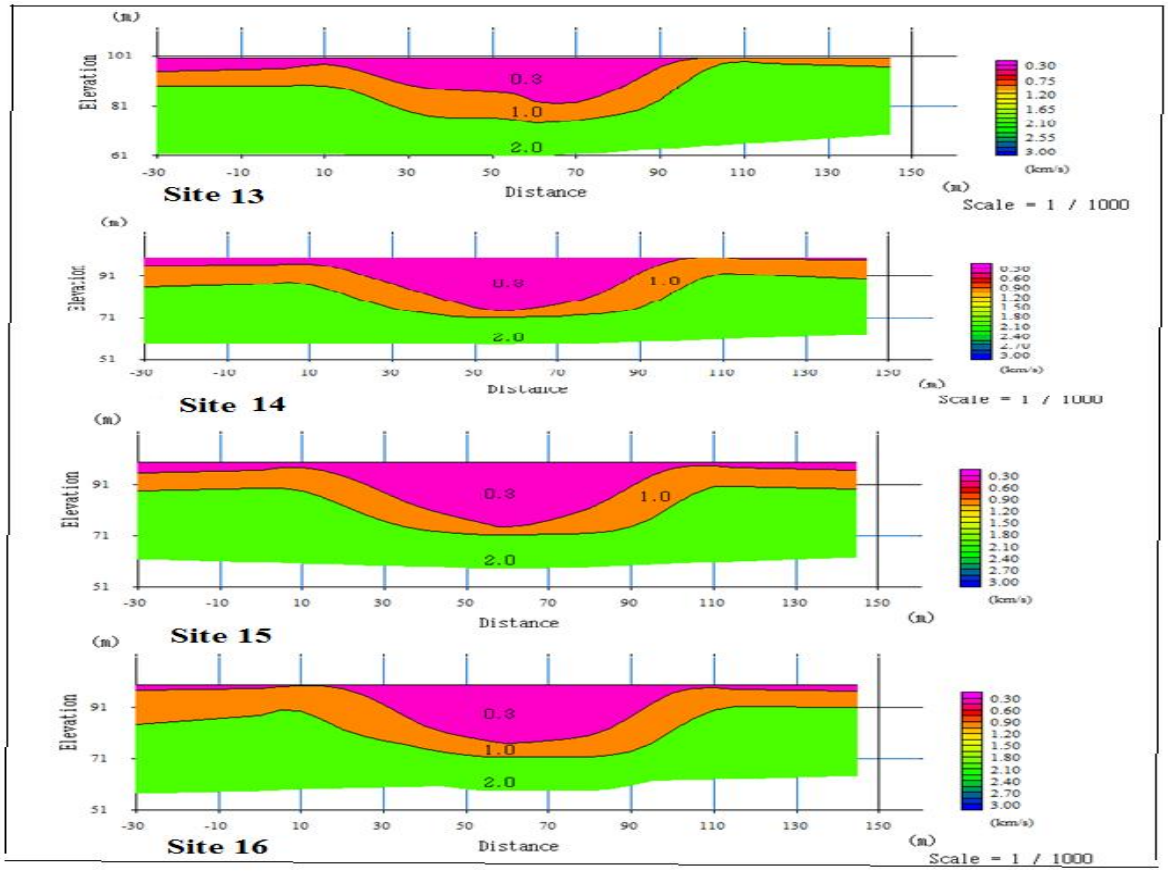
Site 13
Site 14
Site 15
Site 16
Elevation
Distance
(m)
Scale = 1 / 1000
0.3
1.0
2.0
(km/s)

Appendix II: Location, average Vp and Vs of the upper 30m, Vp/Vs ratio amplification factor and site class of the study area.

Site No	Site Name	Latitude	Longitude	Average Vp upper 30 m (m/s)	Average Vs upper 30 m (m/s)	Vp/Vs ratio	amplification factor	NEHRP Vs Soil Profile Type
1	Around Medhanialem Grave	530497	941502	-	382.6	-	1.4	C
2	Behind dero erbata 1	530514	948490	1220	410	2.98	1.38	C
3	Behind dero erbata 2	531162	949299	900	275.4	3.27	1.6	D
4	Lega adi andode or bole mecheresha	531697	948263	897	326.3	2.75	1.5	D
5	At the back of AU(Gendegara)	532385	947643	1285	360.7	3.56	1.44	C
6	Kebele 07 Sole	533014	945088	710	363.1	1.96	1.438	C
7	Gendigara back of Destar school	532040	945176	445	287.6	1.55	1.56	D
8	AU ber	531916	946005	-	519.5	-	1.26	D
9	Adult Center	531448	945810	605	271.8	2.23	1.6	D
10	kebele04 Awash primary and secondary school	531026	945478	810	406.6	1.99	1.38	C
11	Kebele 14	531216	944829	-	371	-	1.43	C
12	Gendegara near Geda No 2	532453	944979	620	310	2	1.52	D
13	Kebele 14 on the high way	532328	944066	1310	481	2.72	1.3	C
14	At St.Yohans Church	532972	943038	1245	400.8	3.10	1.39	C
15	Gabe Saloque	533134	944091	1205	472.9	2.55	1.31	C
16	Near Adama Harar highway	534454	945345	1100	435.9	2.52	1.35	C
17	Along Harar Rail	534692	946367	1225	419.4	2.9	1.37	C
18	Near Welenchity	536502	747442	1050	312.7	3.5	1.52	D

AppedixIII: Lithological log of the study area

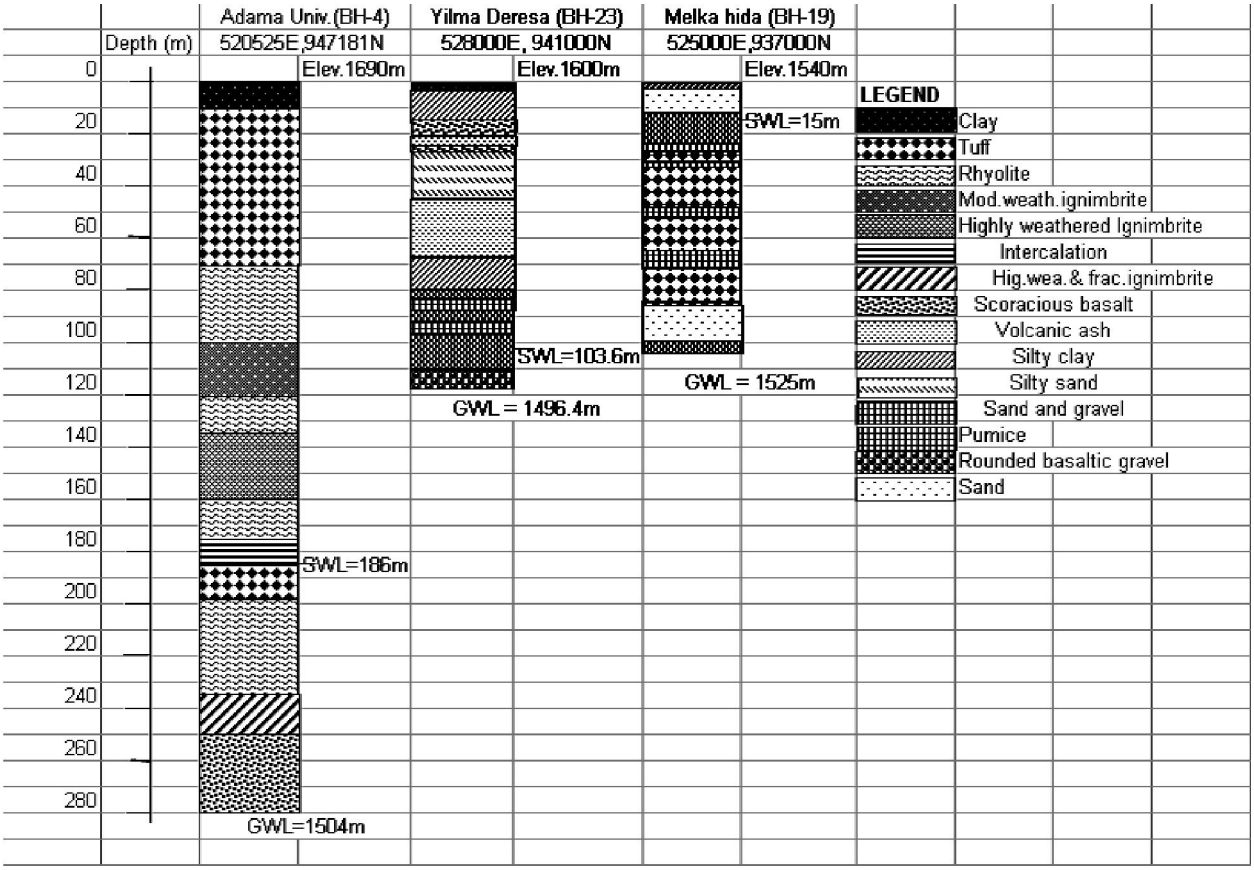

Appendix IV: 1D Shear wave velocity model

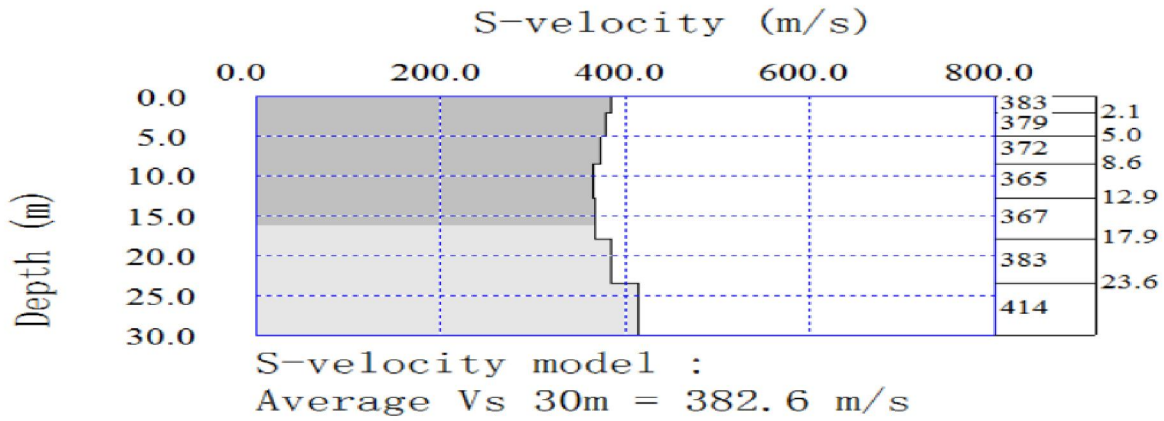

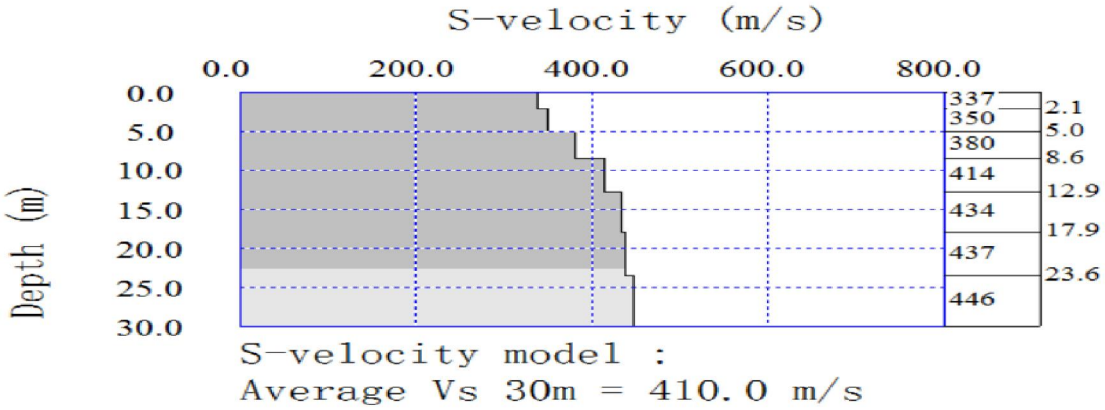

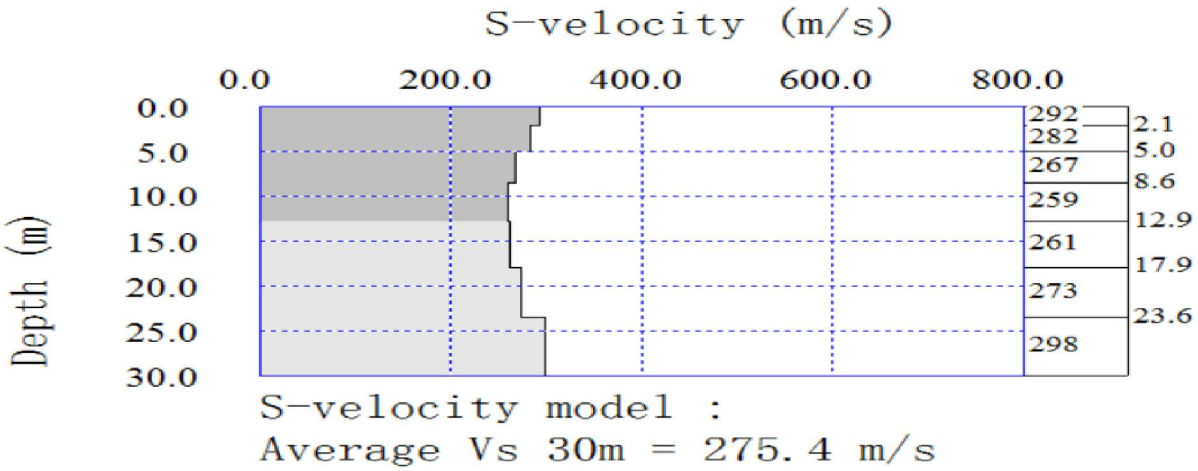

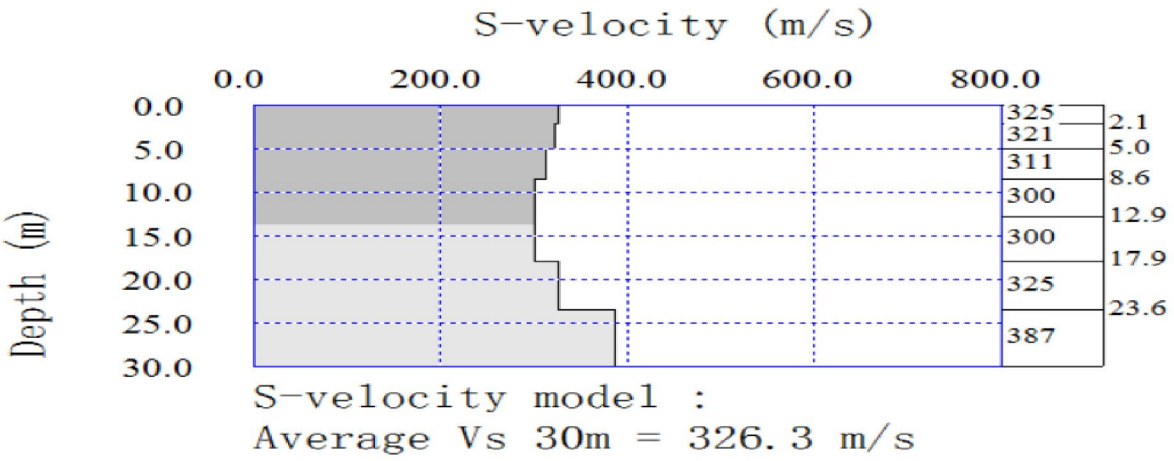

S-velocity model :
Average Vs 30m = 326.3 m/s

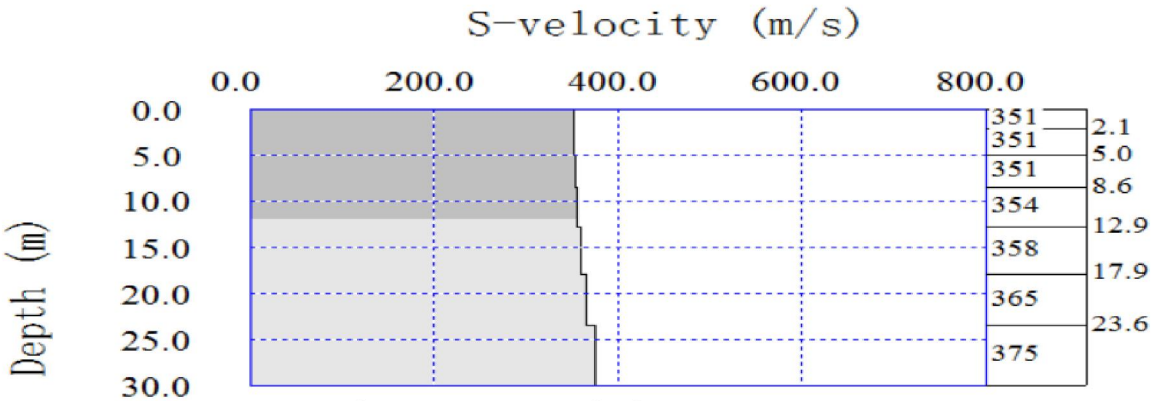

S-velocity model :
Average Vs 30m = 360.7 m/s

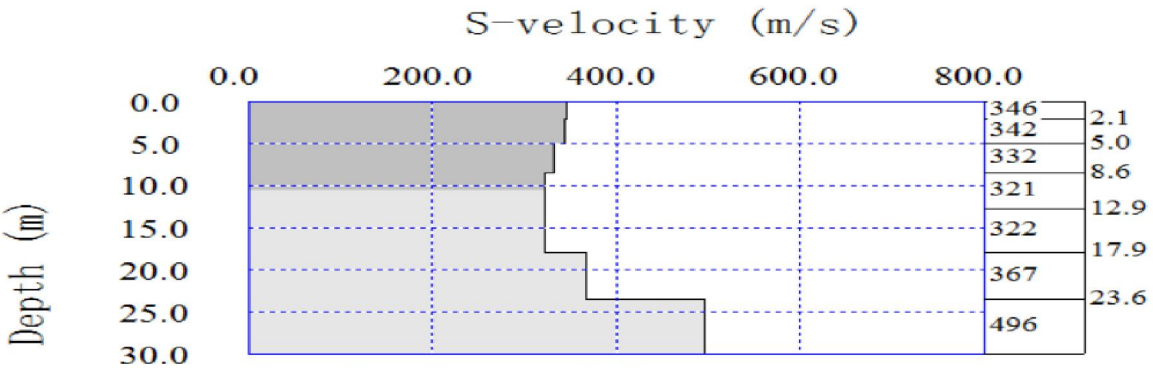

S-velocity model :
Average Vs 30m = 363.1 m/s

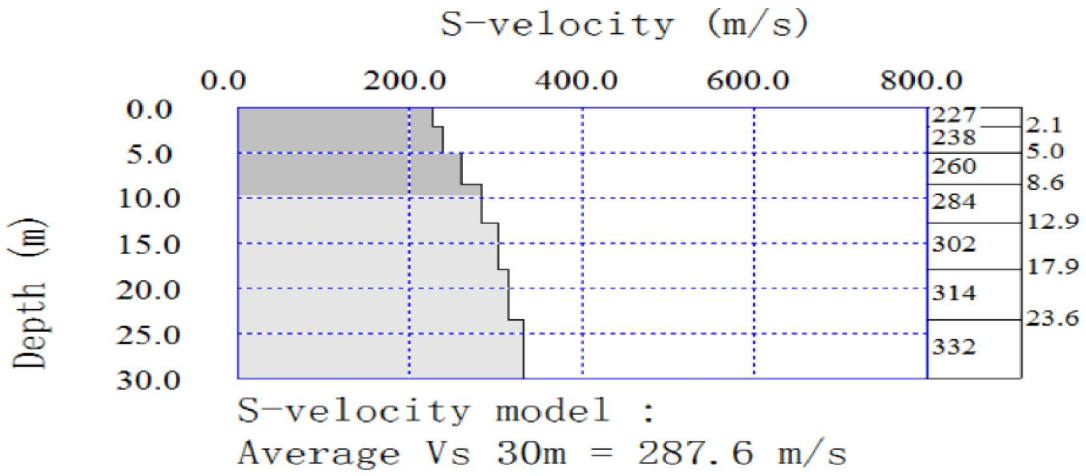

S-velocity model :
Average Vs 30m = 287.6 m/s

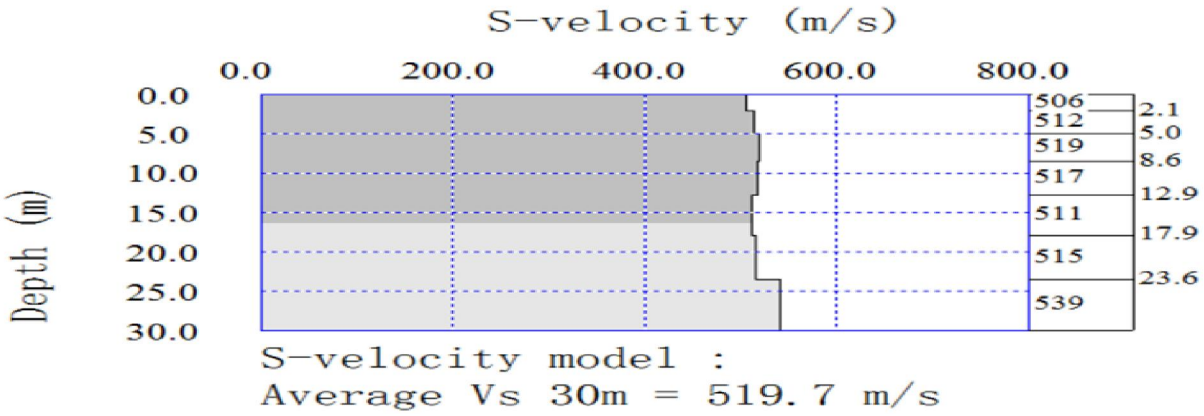

S-velocity model :
Average Vs 30m = 519.7 m/s

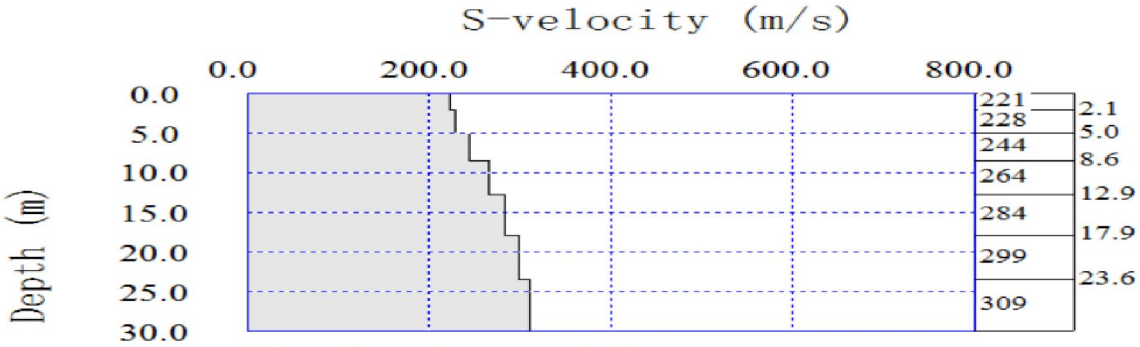

S-velocity model :
Average Vs 30m = 271.8 m/s

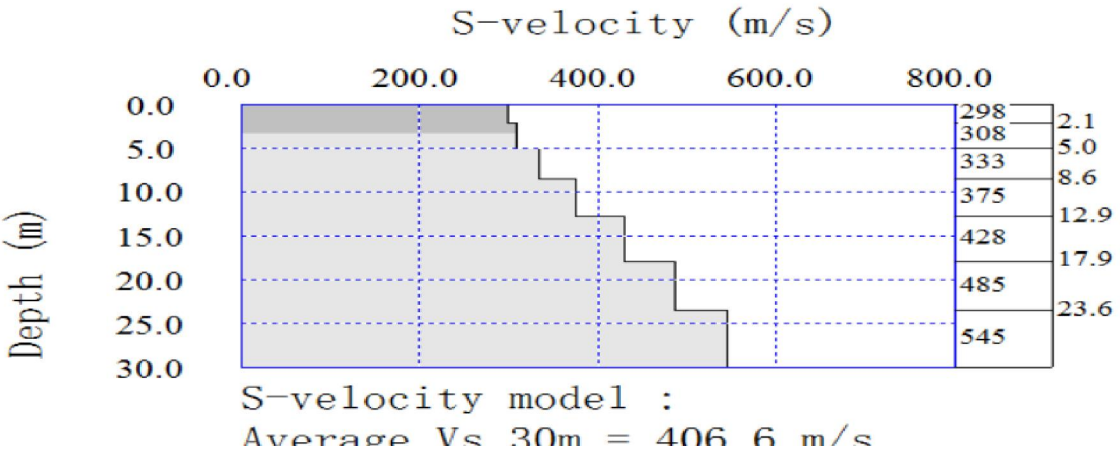
S-velocity (m/s)
0.0
200.0
400.0
600.0
800.0
Depth (m)
0.0
5.0
10.0
15.0
20.0
25.0
30.0
298
308
333
375
428
485
545
2.1
5.0
8.6
12.9
17.9
23.6
S-velocity model :
Average Vs 30m = 406.6 m/s

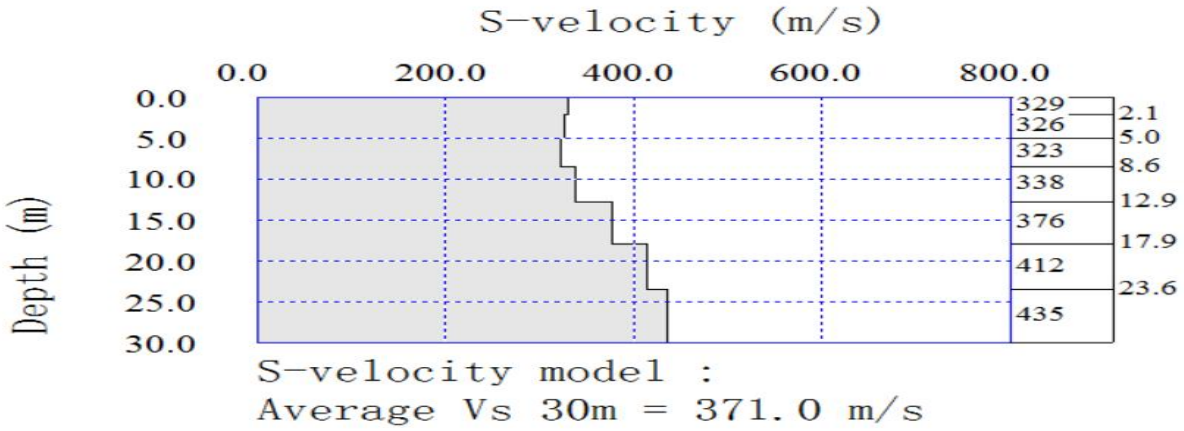
S-velocity (m/s)
0.0
200.0
400.0
600.0
800.0
Depth (m)
0.0
5.0
10.0
15.0
20.0
25.0
30.0
329
326
323
338
376
412
435
2.1
5.0
8.6
12.9
17.9
23.6
S-velocity model :
Average Vs 30m = 371.0 m/s

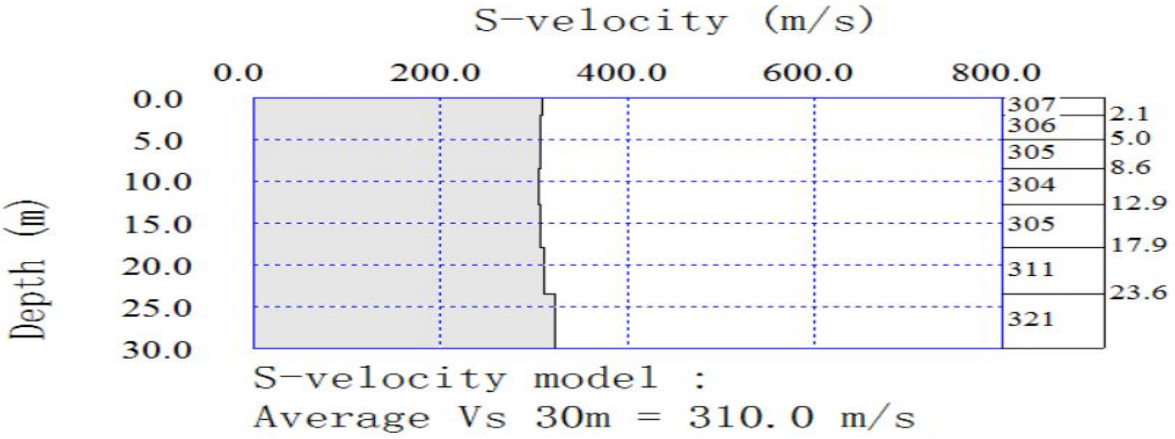
S-velocity (m/s)
0.0
200.0
400.0
600.0
800.0
Depth (m)
0.0
5.0
10.0
15.0
20.0
25.0
30.0
307
306
305
304
305
311
321
2.1
5.0
8.6
12.9
17.9
23.6
S-velocity model :
Average Vs 30m = 310.0 m/s

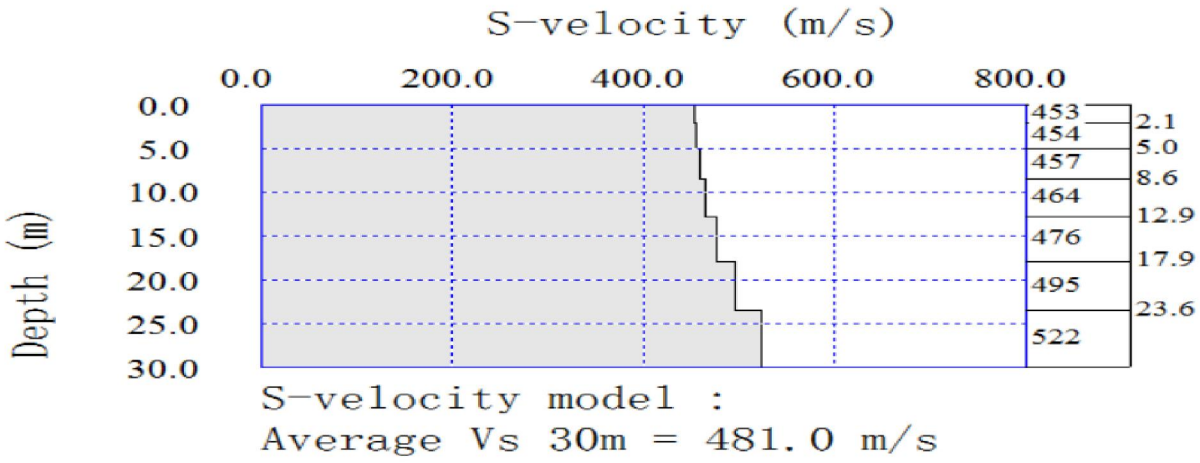
S-velocity (m/s)
0.0
200.0
400.0
600.0
800.0
Depth (m)
0.0
5.0
10.0
15.0
20.0
25.0
30.0
453
454
457
464
476
495
522
2.1
5.0
8.6
12.9
17.9
23.6
S-velocity model :
Average Vs 30m = 481.0 m/s

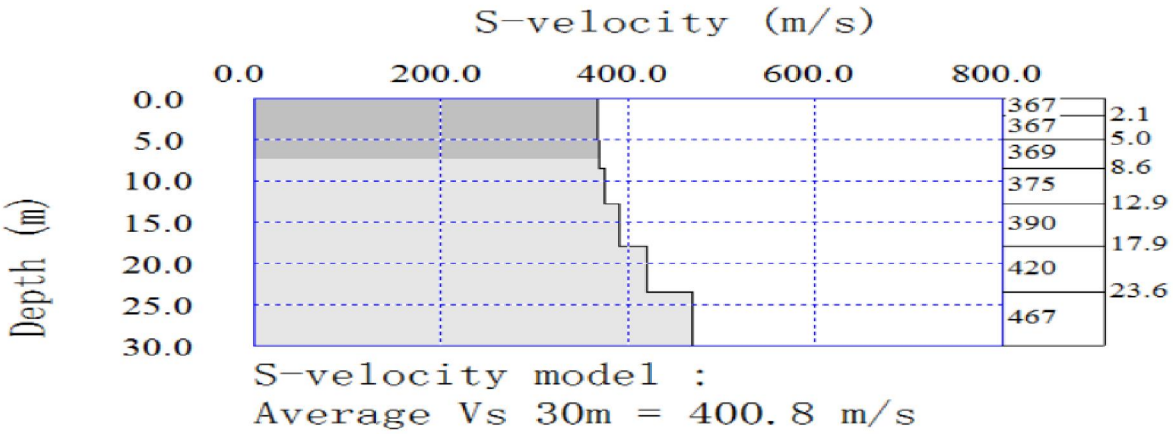
S-velocity (m/s)
0.0
200.0
400.0
600.0
800.0
Depth (m)
0.0
5.0
10.0
15.0
20.0
25.0
30.0
367
367
369
375
390
420
467
2.1
5.0
8.6
12.9
17.9
23.6
S-velocity model :
Average Vs 30m = 400.8 m/s

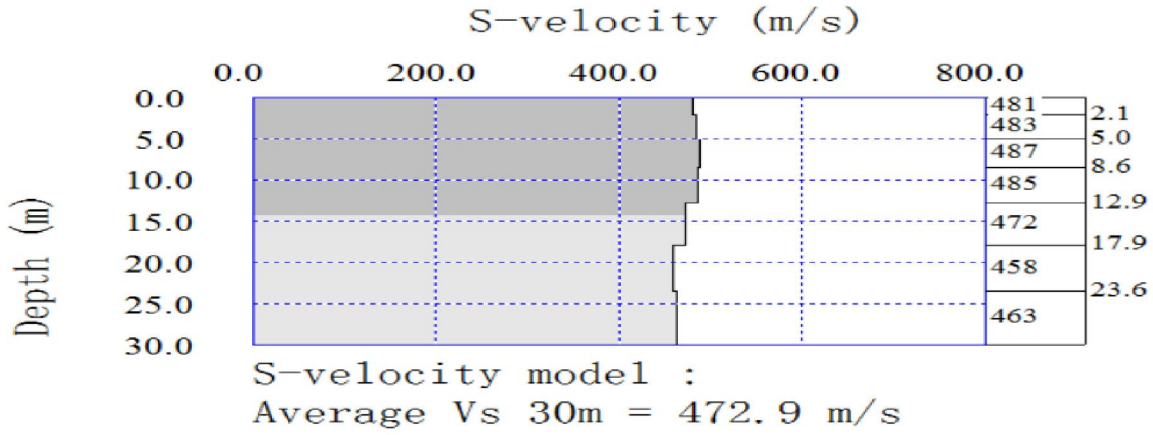
S-velocity (m/s)
0.0
200.0
400.0
600.0
800.0
Depth (m)
0.0
5.0
10.0
15.0
20.0
25.0
30.0
481
483
487
485
472
458
463
2.1
5.0
8.6
12.9
17.9
23.6
S-velocity model :
Average Vs 30m = 472.9 m/s

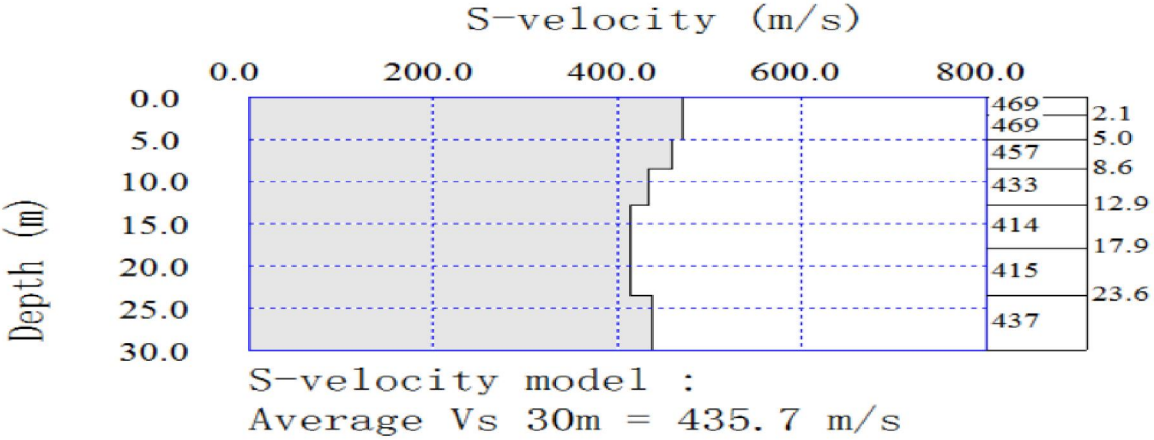
S-velocity (m/s)
0.0
200.0
400.0
600.0
800.0
Depth (m)
0.0
5.0
10.0
15.0
20.0
25.0
30.0
469
469
457
433
414
415
437
2.1
5.0
8.6
12.9
17.9
23.6
S-velocity model :
Average Vs 30m = 435.7 m/s

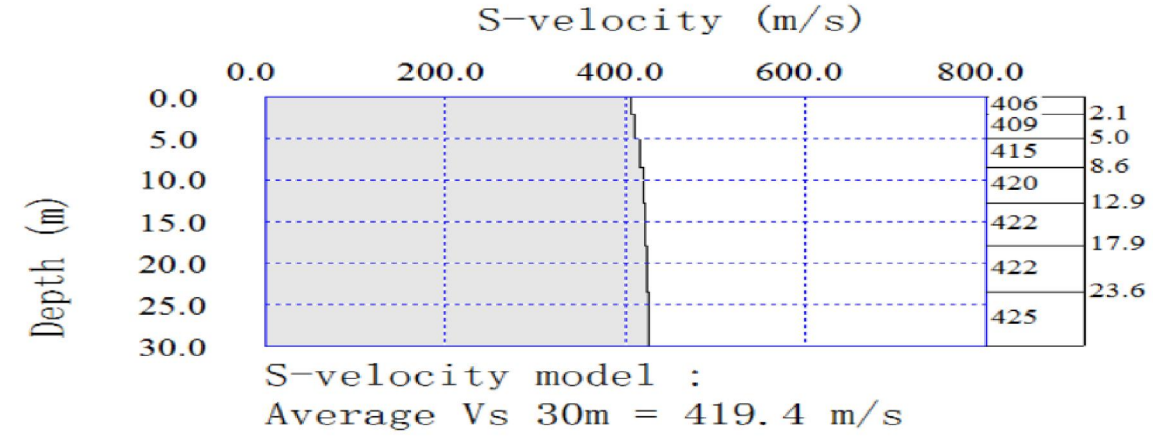
S-velocity (m/s)
0.0
200.0
400.0
600.0
800.0
Depth (m)
0.0
5.0
10.0
15.0
20.0
25.0
30.0
406
409
415
420
422
422
425
2.1
5.0
8.6
12.9
17.9
23.6
S-velocity model :
Average Vs 30m = 419.4 m/s

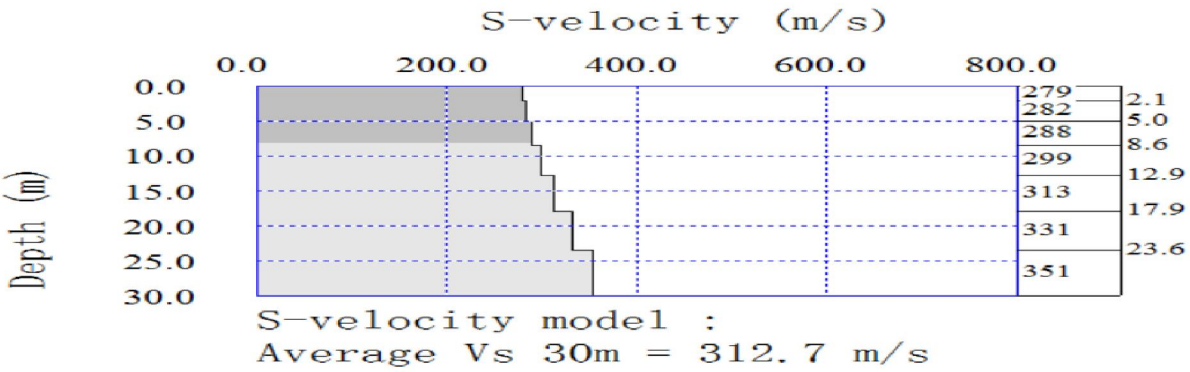
S-velocity (m/s)
0.0
200.0
400.0
600.0
800.0
Depth (m)
0.0
5.0
10.0
15.0
20.0
25.0
30.0
279
282
288
299
313
331
351
2.1
5.0
8.6
12.9
17.9
23.6
S-velocity model :
Average Vs 30m = 312.7 m/s

Declaration

I hereby declare that work which is being presented in this thesis entitled "The role of soil Amplification study in seismic hazard assessment in some selected parts of Adama Town" is performed under the supervision of my research advisor Prof.Tilahun Mammo and it is my original work, has not been presented for a degree or diploma in any other university and that all source of the material used for the thesis have been duly acknowledged.

Freweyni Mekonen

Signature ----------

This thesis have been submitted for examination with approval as University advisor

Advisor	Signature	Date
Professor Tilahun Mammo	----------	----------